Development of Constant-Force Tank-Testing Techniques and Associated Instrumentation

Part II Loadcell Development

Richard William Yemm

A Thesis Submitted for the
Degree of Doctor of Philosophy

The University of Edinburgh
April 1995

Declaration

I certify that the work presented in this thesis, except where explicitly credited to others, is of my own commission in both substance and composition.

[redacted] R. W. Yemm

Abstract

Over the last ten years there has been a resurgence of interest in the detailed experimental testing of sailing yacht designs. Part 1 of this thesis reports work carried out with the aim of improving test realism and data quality. Reduction of the cost of testing by increasing the rate of data generation is also reported.

Constant-Force towing methods in oblique seas were developed. Both Constant-Force and Constant-Velocity data is presented along with a detailed comparison between the two modes. This comparison shows an apparent, frequency dependent, difference of up to +-2% between the two testing modes.

During the work on yacht testing techniques a novel stiff DC loadcell was developed to meet the specific requirements of the tank testing apparatus. Part 2 of this thesis reports the work carried out on the development of this transducer. The final prototype achieved a full scale deflection of 10 microns with an overload factor of more than 20 times the rated load.

Notes on the Layout of this Thesis

This thesis is presented in two separate parts.

Part I reports development of new tank-testing methods for the experimental prediction of yacht performance. This is the main topic of this thesis.

In the course of development of the final towing system there was a requirement for a very stiff loadcell. After assessing various options it was decided to develop a custom loadcell in-house. This took longer than expected and as such has become a major part of the overall project. The definitive loadcell prototype was used in the final towing system.

Part II of this thesis reports the development of the custom loadcell. A patent has been applied for so the information contained in Part II is of a commercially sensitive nature. For this reason the two parts are bound separately in order that Part II can be put on restricted access until the patent application has been processed.

All Figures are at the end of the appropriate Chapters.

Table of Contents

List of Figures

Frontispiece

The photograph overleaf shows the various test, assembly and prototype components described in Part II of this thesis.

In the centre (black anodised) is the testblock used for development and assessment of the optical system. Note the block deflection spring, pivot pin, torque arm and the holes forming the parallelogram spring system.

Clockwise from the foreground:

The final loadcell and miniaturised conditioning circuit used extensively in the towing system reported in Part I of this thesis. Note the parallelogram spring system, eccentric emitter can with its pinch block clamp and the special alloy mounting studs for coupling the unit to the towing system.

Next is the first loadcell prototype, functionally of identical configuration to the testblock.

Continuing clockwise Loadcell #2 with its assembly jig. This jig was also used for assembling and aligning Loadcells #3 and #4 seen alongside.

Next to these is the unassembled Loadcell #5 using a cantilever beam arrangement, single piece aluminium alloy body and eccentric opto mounting pin and can.

In front of this is Loadcell #6 which used similar opto mounting techniques but within a cylindrical stainless steel case similar to the previous prototypes.

Finally, Loadcells #7 and #8 using the symmetrical parallelogram spring system, one piece alloy casing and eccentric can opto mounting. Note the simple construction, screw clamps for the opto cans and the awkward high aspect ratio cuts made possible by EDM.

Chapter 1. Introduction & Aims

1.0 Chapter Breakdown

Chapter 1. sets out a review of the field of force measurement and discusses the various specific requirements of the loadcell for the towing system. The Chapter then justifies the decision to make a custom loadcell tailored to the needs of the towing system.

Chapter 2. reports the alternative technologies considered for the custom loadcell, concluding with a decision to evaluate the potential of a loadcell using optical techniques.

Chapter 3. outlines the initial design study carried out to assess the potential of the optical loadcell, leading to a provisional design.

Chapter 4. describes testing of the optical system to be used in the loadcell prototypes and how these tests influenced the design of the first prototype.

Chapter 5. describes the prototype development programme and includes details of the performance of the various configurations.

Chapter 6. concludes the work on the optical loadcells and makes recommendations for future work.

1.1 Chapter Summary

Part 2 of this thesis begins with a very brief introduction to the history of force measurement. The specific loadcell requirements of the towing system are summarised. The chapter then moves on to assess the suitability of a range of commercially available loadcells. With several shortfalls identified alternatives are discussed.

The chapter concludes with a decision to assess the potential for making a custom loadcell to meet the towing system requirements.

1.2 Introduction

The requirement for accurate, repeatable measurement of weight for the bartering and selling of goods goes back many centuries. This led to the development of weighing scales and spring balances of many forms.

Developments in force measurement were given new impetus in the middle of this century in parallel with rapid developments in the world of electronics. The application of fine wire to the measurement of strain was established in the USA during the Second World War. Although other techniques have been used, strain gauge technology in its various forms now dominates this area of test and measurement.

Modern requirements for accurate, stable and stiff loadcells for test and measurement and process control applications have led to a vast range of commercially available force measurement systems.

1.3 Requirements for Towing System Loadcell

The loadcells for the towing system had a number of important requirements.

The pushrod drives had been carefully designed to eliminate low frequency mechanical resonances to increase the available feedback loop gain. A target for the first resonance within the drive loop of over 750 Hz was set. This was achieved for the mechanical components within the system, the critical element was now the loadcell. The moving mass between the drive motor and loadcell was estimated at approximately 1 kilogram. Thus the required stiffness was calculated to be 20 MN/m. With a load range of +-50 N this translates into a full scale deflection of +-2.5 um.

Other requirements included; tension and compression operation, D.C. coupling, isolation of off-axis loads and bending moments, good short/long term stability, high overload capacity, small size and weight, and low cost.

These performance criteria proved to be well outwith the capabilities of any loadcells owned by the Wavepower Project. Thus a search of commercially available loadcells was carried out.

1.4 Review of Current State of the Art Loadcells

Figure 1.1 shows a table summarising the specifications and characteristics of typical stiff D.C. coupled loadcells available from three major manufacturers; Entran, RDP and Maywood Instruments Ltd. A much wider search was carried out but the models included in the table are representative of the best performance available.

1.4.1 Entran Devices Ltd.

Entran produce a large range of loadcell types and characteristics. They seem to concentrate on miniaturisation and stiffness producing the smallest package sizes available. However, this means that most of the range do not include off axis load isolation. Linearity, hysteresis and temperature stability are generally good. Semiconductor strain gauge technology is used throughout the product range. Overload capacities are in the range 1.5 -2 with the exception of the ELJ-N Series. The ELO-06 range is included mainly for interest. It was the only cell commercially available which met the stiffness target. It is however a compression only unit. Possible application of this cell in the towing system is discussed later.

1.4.2 RDP Group

RDP again produce a wide range of strain gauge loadcells. The emphasis is more on accuracy and stability than miniaturisation. All models within their range include isolating flexures to reduce the effect of off axis loads and moments. This means that their cells are generally much larger than those available from Entran. Claimed performance figures are generally slightly better than given by Entran. Overload capacities are 1.5 times the rated load.

1.4.3 Maywood Instruments Ltd.

Maywood seem to concentrate almost exclusively on performance. As with the RDP range, off axis loads are isolated. Quoted performance figures are generally the best available. These have been obtained by sacrificing stiffness and increasing package size. Full scale

deflections are several factors greater, and case dimensions are generally an order of magnitude bigger than Entran equivalents. All models still use some form of strain gauge technology. Once again overload limits are 1.5 times rated load.

1.4.4 Summary

Commercially available loadcells clearly show the performance trade-offs typical of strain gauge systems.

All performance figures are inversely proportional to both full-scale deflection and package size. Linearity and hysteresis in particular seem very sensitive to the size of the deflecting members in relation to the gauge size.

Miniaturisation is generally achieved only at the expense of off-axis load isolation. This may prove to be a false economy for many applications.

High stiffness along with high strain sensitivity lead to typical overload capacities of less than a factor of two times the rated load. This makes most strain gauge loadcells inherently fragile. Protection against accidental damage is often achieved by choosing a cell with a rated load much greater than required for normal operation. This has the detrimental effect of correspondingly derating the rest of the performance specifications.

Larger deflections allow the use of positive endstops that can increase overload factors to between 5 and 10 as with the Entran ELJ-N Series.

1.5 Suitability of Commercial Units for Towing System

As can be seen in Figure 1.1 only the ELO-06 range have the required stiffness. However, these are sub-miniature compression only cells, achieving high stiffness by extreme miniaturisation. This limits the maximum load range to 0-100N. In theory the unit could be pre-loaded to 50% full range. This would require a system capable of adjustment to less than 1um. This mechanism must have the same thermal expansion characteristics as the loadcell or the already relatively poor thermal, linearity and hysteresis characteristics may be compromised further.

The best options overall seemed to be the Entran ELF-13 or RDP 11 Series. The Entran cell would provide the highest stiffness, although this would still be a factor of five below the target. The RDP cell would be a factor of 10 off the target. A carefully designed off axis support would be required for the Entran cell, although less critical than for the ELO-06 model. The RDP cell could be used directly.

Both of these units are very expensive. At around £600 each (1991 prices) they were both out of reach of the available budget.

Overall it was deemed that the current state of the art commercial loadcells were not suitable for use in the towing system.

1.6 Other Options

This survey led to a general review of alternative options.

One way of achieving the required stiffness target would be to simply use a loadcell of far greater load range as mentioned above for increasing overload capacity. This would be unsatisfactory because again signal to noise

ratio, temperature drift and other sources of error would be amplified by the same factor.

The target specifications could easily be met using one of several ranges of piezoelectric loadcells. These use the piezoelectric properties of some crystalline solids to generate a charge proportional to applied load. This charge is converted to an output voltage using a "charge amplifier". No such circuit can be made perfectly "charge-tight" with the result that this type of cell is only suitable for measuring reversing or quasi-static loads. The towing system requires static force measurement. It may be possible to build a charge amplifier with a sufficiently long time constant to be of use in the towing system. A sophisticated system may be able to correct for charge leakage via the control computer and accurate calibration. Another option may be the use of the piezo loadcell to close the main feedback loop, D.C. coupling would be superimposed using a low stiffness strain gauge cell in series to allow the computer to output "leakage compensated" demands. Determining the stability of such a set-up would be a difficult task, however it was kept in mind while other options were examined.

The other option was to try and make a custom loadcell in-house tailored to the towing system specifications.

1.7 Conclusions and Aims

It was concluded that the best way forward was to examine the possibilities of making a loadcell in house. If this could be achieved the unit would almost certainly find commercial application.

The Entran ELF-13 would be chosen if this study was to prove unsuccessful. Extra funding would have to be sought in the event of this choice being made.

In the event of insufficient funds being available, the piezo loadcell options would be examined.

Manuf'er	Model	F.S. Defl'n	Max. Ov'ld	Isol. Flex ?	Technol.	Load Ranges	Lin'ty	Hyst.	Temperature			Case Dims.
									Range	Zero	Gain	
Entran	ELF-13	13	1.5	No	SCSG	5-500	+-1	+-1	-40,120	0.02	0.05	Cyl. 12.7x2.5
Entran	ELF-26	13	2.0	No	SCSG	10-10000	+-1	+-1	-40,120	0.02	0.02	Cyl. 25.4x5.0
Entran	ELH-11	20	2.0	No	SCSG	10-750	+-0.5	+-0.5	-40,120	0.02	0.04	Cyl. 10.0x10.0
Entran	ELJ-N	80	10.0	Yes	SCSG	0.2-5	+-0.5	+-0.5	-40,80	0.02	0.05	20x7.5x7.5
Entran	MLG	25	1.5	Yes	SCSG	50-1000	+-0.1	+-0.05	-40,100	0.01	0.01	25.4x41x17
Entran	ELO-06	2.5	2.0	No	SCSG	5-100	+-2.0	+-1.0	-40,120	0.04	0.05	5.0x10.0x2.0
RDP	31/34	25	1.5	Yes	F/SCSG	0.5-20000	+-0.15	+-0.15	-50,120	0.01	0.03	Cyl. 25.0x15.0
RDP	11	25	1.5	Yes	F/SCSG	0.5-2000	+-0.5	+-0.5	-50,120	0.02	0.02	Cyl. 12.5x7.0
Maywood	U4000	?	1.5	Yes	SG	10-50000	+-0.04	+-0.015	-20,80	0.002	0.002	75x48x40
Maywood	B4000	80	1.5	Yes	SG	0.5-20	+-0.1	+-0.1	-20,80	0.02	0.01	110x35x21

F.S.Defl'n (In microns), Max Ov'ld (x Rated Load), Technology (SCSG: Semiconductor Strain Gauge, FSG: Foil Strain Gauge), Load Ranges (Newtons) Linearity, Hysteresis, Temperature Drift (% Full Scale Output (per °C)), Temperature Range (°C), Case Dimensions (millimetres).

Figure 1.1 Summary of Typical Commercial Loadcells

Chapter 2. Alternatives Considered

2.0 Chapter Summary

This chapter looks at various alternatives for making a loadcell tailored to the specifications laid down in the previous chapter. Conventional strain gauge methods are first studied followed by a brief discussion of various alternatives considered. The chapter concludes with a positive decision to evaluate the potential of a loadcell based around an optical measurement technique.

2.1 Evaluation of Competing Technologies.

The lack of a suitable loadcell from commercial sources led to a study as to whether a custom unit could be made, in house, to meet the required specification. This study began with an evaluation of several technologies to determine the most suitable measuring technique.

2.1.1 Strain Gauge Techniques

As discussed in the previous chapter, conventional loadcells almost exclusively use some form of strain gauge technology. The strain in a deflecting element is measured using the piezo resistive properties of certain materials. The such materials are usually supplied in the form of a prefabricated strain gauge, ready for bonding to the substrate. The strain sensitivity of the gauge material is usually quantified using a term known as the "Gauge Factor". This is simply the ratio of change in resistance with respect to the applied strain.

There are two main types of strain gauge in common use. Metal foil strain gauges, and semiconductor gauges. The latter is a more recent development with much higher strain sensitivity. However it has significant drawbacks as discussed later. A full description of all types of strain

gauge technology and their application can be found in [1,2,3,4].

Metal foil gauges have a low sensitivity to applied strain, with typical gauge factors of around two. This means that the deflecting element of the loadcell must be heavily strained to give a reasonable output. They are also susceptible to fatigue problems. They are, however, easy to use and inexpensive. Automatic temperature compensation is available for various substrate materials. The strain sensitivity of foil gauges is insufficient to build a loadcell to meet the target stiffness.

The higher strain sensitivity of semiconductor gauges (gauge factors between 100 and 150), is largely offset by poor linearity characteristics and very high temperature coefficients. Many manufacturers use this technology for stiff loadcells but they are expensive and despite complicated conditioning and temperature correction circuitry remain sensitive to temperature and linearity problems.

A vast amount of development has already been carried out to optimise the performance of this technology and therefore current state of the art units are unlikely to be significantly improved unless there is a further development in gauge technology.

The Entran and RDP loadcells discussed in the previous section are typical of the performance available. Stiffness has had to be sacrificed to improve the other qualities. The maximum stiffness does not meet the required specification.

2.1.2 Alternative technologies considered

The review of the potential of strain measurement techniques revealed that a different approach would have to be adopted. The other common way of measuring load is to directly measure the linear deflection of a member, as in the everyday spring balance. To make a loadcell of the required stiffness a measuring system with a full scale range of around a 2.5 microns is required. This translates into a system resolution of around 2.5 nano-metres with a signal to noise ration of 1000. Several different methods were examined.

2.1.3 Linear Variable Differential Transformer (L.V.D.T)

The L.V.D.T is a well established method of measuring linear motion. It is a very versatile instrument with measuring ranges available from over a metre down to fractions of a millimetre. A movable ferrite core is used to vary the magnetic path between a central excitation coil and two peripheral secondary coils. The output from these coils is demodulated and the difference taken to give an output proportional to the core position. They are extremely rugged and have excellent immunity to various misalignments. A full review of L.V.D.T. characteristics and performance can be found [1,2,3,4].

To evaluate whether this method was capable of giving the required resolution, relevant literature [1,2,3,4] and commercial modules were studied. Several manufacturers produce units with full scale ranges of +-1mm, but at best these have a resolution down into the tens of nanometre range, which is insufficient.

Due to the modulated nature of the raw output signal, the dominant source of output noise is the residual ripple left after rectification and smoothing. Most manufacturers

reduce this to an acceptable level by severely restricting the bandwidth and by raising the excitation frequency. The former is unacceptable in this application and the excitation frequency is ultimately limited by the inductance of the coils.

Production of very small coils is expensive, and the conditioning circuitry is of necessity complex.

2.1.4 Inductance/Reluctance

Various manufacturers offer ranges of non-contacting displacement transducers using inductive techniques. A radio frequency signal is fed into a coil in the tip of the transducer. This induces eddy currents in any conducting surface in close proximity. As the coil/target distance reduces the eddy current losses increase leading to a parabolic voltage output with respect to separation. Most commercial units linearise the output signal over a fixed displacement range. Once again the subject is discussed in detail in [1,2,3,4].

Typical units are made by Graham & White Instruments and Keyence Ltd. Typical resolutions are quoted as being in the order of 100nm. This would translate into a full scale range of around 0.1mm with a signal to noise ratio of 1000. Again this does not meet the required stiffness specification.

It may be possible to make a unit that increases the available resolution. This would probably be a complex process with the complete unit probably ending up very bulky. Once again very small coils are required. However, this technology was kept in mind until the choice to go the optical route was made.

2.1.5 Capacitance

The use of capacitive methods for measuring small displacements is common. Neubert[1] gives a particularly full description of this method of displacement measurement. Of special note is the section on construction of the variable capacitance elements and the associated problems. Several capacitive proximity sensors are commercially available. The output from capacitive systems is prone to linearity problems [1,2]. These may be reduced by using a differential pair as shown in [1]. However, very small gaps would be required posing serious alignment difficulties. Again there may be signal demodulation problems.

2.1.6 Hydrostatic Pressure Sensing

One of the most promising ideas studied was the use of a miniature commercial pressure transducer to measure the pressure in a hydraulic lock formed behind a load diaphragm. The volume change within typical miniature pressure cells would be negligible when compared with the compressibility of the working fluid.

The system would be prone to thermal expansion related drift and barometric effects unless a differential configuration was used. Various working fluids were considered. Glycerol was a prime contender with its high bulk modulus of rigidity and low thermal expansion. For ultimate performance mercury was considered.

This elegant idea seemed very promising. However, several problems may prove serious. Any trapped air within the system would cripple the stiffness necessitating careful filling. This would be done by evacuating the unit before introducing the working fluid. Very exacting sealing would be required to prevent air ingress in operation. Extreme

care would be required to ensure that the surrounding deflecting mechanism did not impart significant parasitic load as the hydraulic cell expanded or contracted.

Stiffnesses were estimated by neglecting the volume change of the pressure transducer and assuming a fluid cavity 25mm in diameter with a depth of 1mm. Full scale deflections of less than 4 nanometres should be possible using mercury, derating to approximately 25 nanometres for glycerol as a working fluid.

Again this idea was kept in mind while alternatives were studied.

2.1.7 Force Balance Methods

Another method of making stable, low deflection force transducers is by using an active force balance system. Any of the displacement measuring techniques discussed above can be used to generate a position error signal. This is amplified and used to drive an electro-mechanical force coil. This method is treated in much detail in Neubert[1]. The technique promises very high potential stiffnesses. Also the unit would be largely immune to instability and drift in all elements apart from the force coil [1]. However, to improve the transient response of the system, velocity information is required in addition to position. This in conjunction with provision for the force coil itself mean that size and weight will increase markedly. The wide bandwidth required for the towing system loadcell may well compromise the D.C. performance markedly.

2.1.8 Optical Techniques

Before explaining the optical technologies considered a brief introduction to the project which initially inspired investigation of this technology. Professor Stephen Salter, Edinburgh University Wavepower Project (EUWPP) and Dr. Tom Stevenson, Electrical Engineering, University of Edinburgh were involved in the collaborative ESPRIT 2048 project funded by the EEC. Also working on this contract were David Jeffery and Jon Muhl, EUWPP. The project involved development and testing of a range of instrumentation technology. Part of the work carried out for ESPRIT 2048 by David Jeffery and Jon Muhl was of direct relevance to the loadcell project reported in this thesis.

The method finally chosen was inspired by an optical position measurement system developed for the ESPRIT 2048 project suggested by Tom Stevenson. This used the motion of a simple opaque vane to induce differential shuttering of two emitter/receiver pairs. The optical components used near infrared wavelengths of the order of 900nm. There is a vast range of components available in this field, they are used extensively in fibre-optic applications. They are simple, cheap, rugged and easy to use. The unit developed for the ESPRIT 2048 contract had a resolution of around 50 nm. Full details of the performance of this system is given in the ESPRIT 2048 final report.

This resolution was insufficient for the required loadcell stiffness so alternative shuttering methods were considered. The resolution can be increased dramatically if two opposing gratings are used in place of the vane. The use of such gratings for the generation of Moire and vernier fringes for long throw position measurement is commonplace. Such applications are discussed in [5,6]. Peter Woodhead pointed out that optimum short range performance would be with the gratings parallel. If the one of the gratings incorporates a 180 degree phase shift

between the tow pairs of emitters/receivers a differential, push/pull system will be retained. System resolution would now be limited only by choice of grating pitch, collimation imperfections and diffraction effects.

A brief evaluation of the potential of such an optical system was carried out and is described below.

Assuming the same signal to noise ratio of 5000 achieved with the ESPRIT transducers, a system resolution of 2.5nm would require a full travel motion amplitude of +-10um. This means that the target specification could be met using gratings of 40um pitch, or 25 lines/mm. This should be clear of serious diffraction and collimation problems as discussed in [5,6]. The results from David Jeffrey's study of the opto switches seemed to indicate that thermal drift should be very low due to the differential configuration.

Thus it was concluded that the optical method was the most promising of all the ideas evaluated and was worthy of further investigation. Further applications of the use of optical systems for displacement measurement are discussed in [5,6].

2.2 Conclusions

The evaluation of alternatives to strain gauge technology for the development of a stiff loadcell threw up a number of interesting alternatives.

The most novel idea was the use of a hydraulic lock in conjunction with miniature pressure transducers. It was felt that although this technique promised the highest stiffnesses there were too many unknowns to proceed. The idea was none the less kept in mind for possible future study.

Optical techniques using infrared components and fine gratings seemed to offer a comparatively simple, cheap solution to the problem. The grating pitches envisaged were conservative compared to existing applications and it was expected that development of a system with the required resolution should give few problems.

Therefore the decision was made to undertake a full evaluation, design and testing programme, with the aim of developing a new generation of stiff D.C. loadcells using optical displacement measurement.

Chapter 3. Feasibility Study

3.0 Chapter Summary

A discussion of the various factors considered in the design of the optical system components, deflecting mechanism and conditioning electronics is presented. Provisional designs for these elements are described.

3.1 Optical System Components

3.1.1 Gratings

The gratings are the most important element of the design. For the success of the idea, efficient shuttering is a must. This calls for dimensionally consistent and stable line structures, with a high contrast between clear and opaque. The grating substrate should be as thin as possible, to maximise the current transfer ratio.

Several options for grating manufacture were considered. The original plan was to photographically reduce hand drawn gratings, then use the negatives in the optical system. This crude approach was the original method used by physicists studying diffraction effects. With careful setting up reasonable results are possible.

With concerns over the dimensional accuracy and stability of such gratings, I was referred to Tom Stevenson, from the Electrical Engineering Microfabrication Unit for advice.

The EMF Unit has an optical pattern generator for the sole purpose of generating gratings. The grating pitch, orientation angle and overall dimensions can be set up. Phase shifts in the pattern are also possible. The pattern generator exposes a photographic emulsion on a 1/16" glass substrate. The system is capable of generating patterns down to the resolution of the photographic emulsion used.

The original intention was to contact print the master gratings onto ordinary film to reduce thickness. The gratings would then be bonded to the opto devices, and would thus rely on them for flatness and dimensional stability. After consideration it was decided that a better course of action would be to use the glass gratings directly. The extra thickness penalty would be offset by vastly improved shuttering performance.

There is also a facility for cutting the gratings to size using a diamond slitting saw.

Other methods considered for grating production included etched metal shim and microfabrication techniques on a silicon substrate. Both of these approaches are more complicated and expensive than the glass grating option. They would be strong contenders for a production loadcell, where set up overheads can be recovered over a large run.

The optimum grating pitch can only be determined experimentally. There are several factors that will determine the best solution.

For coarse gratings, fewer than 10 lines/mm, diffraction and imperfect collimation of the light source have little effect on the shuttering efficiency [5]. The wide lines and spaces would be reproduced with a high contrast by the pattern generator and emulsion. With gratings of this type, working with a small gap, signal modulation should be close to 100% of the light/dark range. However, the large grating pitch will require a large deflection.

The shuttering efficiency of the finest gratings, 50-100 /mm, is dominated by diffraction losses and collimation imperfections [5,6]. The fall off of signal modulation is rapid with increasing grating separation. However, the small pitch gives a short full range throw.

At a certain pitch, to be determined experimentally, these various factors will combine to give a maximum deflection sensitivity. This would be chosen as the operating configuration of the optical system for the loadcell.

3.1.2 Infrared Components

Various different IR components were considered, the main criteria being; small size, collimation performance, convenient lead connections and low cost.

Small size and lead configuration are vital if the loadcell is to be compact. It does not matter how small the opto device itself is if the leads come off at awkward angles.

An extensive search of the market was carried out to assess what was available. Data was collected from many manufacturers and distributers including; RS, Farnell, Hewlett-Packard, III-V Systems, Isocom, Telefunken, Harris and Honeywell. This database of components was very useful for choosing the best optical components for the various mechanical layouts studied.

3.2 Mounting of the System Components

The mounting of the system components has three main requirements. The infrared devices must be well aligned, securely mounted and protected from damage and stray light. The gratings must be well aligned in every respect if efficient symmetrical shuttering is to be achieved.

If alignment cannot be guaranteed during assembly, provision has to be made for appropriate adjustment after assembly.

Several different alternatives were considered to achieve the necessary alignment. These are inexorably linked with the mechanical layout of the loadcell and as such will be discussed in parallel with mechanical design in the following section.

3.3 Mechanical Ideas/Layouts

All load cells are based around some form of deflecting structure, the deformation of which is measured, by whatever means, to quantify the load. The deflecting mechanism to be used in an optical loadcell will have several important differences from a strain gauge system.

Since the deflection is being measured directly and not by measurement of strain within the material, no provision has to be made for mounting the usually large strain gauges. For a strain gauge loadcell to work with maximum efficiency, the gauge has to be mounted, for example, at the root of a long beam, where the bending moment is largest. Thus, the overall size of the loadcell is great compared with the discrete gauge. This means that opto loadcell body should be inherently more space efficient than rival systems.

The gratings and opto pairs are susceptible to being knocked out of alignment. Stray light from outside sources will lead to large measurement errors. Any contamination of the gratings will lead to a degradation of the optical performance. Due to the small operating clearances envisaged, dust or dirt build up in the system will eventually cause friction and stiction, again leading to errors. All of these point towards a totally enclosed layout, not required in conventional loadcells.

Components require, and need to maintain, accurate alignment, unlike the "stick on and go" strain gauge

technology. All components need to be very accurately made with absolutely no chance of slippage or slop causing errors. Unless carefully designed this will raise the cost of the loadcell dramatically.

With a strain gauge cell only the deflection of the instrumented portion has to be linear. Nonlinear, secondary deflections in the opto loadcell will read as non-linearities on the output. Again a careful approach to design is required.

The problem of crosstalk due to off-axis loads and bending moments is common to both technologies. However, they have to be dealt with in different ways. With strain gauge systems full Wheatstone-bridge methods can be used in most of cases to reduce this problem. However, most high accuracy loadcells also include mechanical isolation to increase overload capacity in addition to improving performance. The opto system will give virtually zero output for deflections parallel to the grating lines, but may suffer badly in other modes. Thus some effective form of mechanical off-axis load isolation will be vital.

With these factors in mind different layouts were studied.

3.4 Structural Configurations

Two main configurations were looked at in detail.

3.4.1 Parallelogram Spring

A simple general purpose parallelogram deflecting mechanism is shown in Figure 3.1. It consists of a solid block with four holes drilled in it, two on each side. Diagonal saw cuts free the block to deflect as a parallelogram.

The system possesses good off axis stiffness due to the depth of the individual springs and the parallelogram layout. It can be made from a single block of metal and involves few high tolerance machining operations. This arrangement is thus easy and cheap to make.

However, the layout is inherently awkward for an axial loadcell design. The unit is still bulky with the spring system still the largest entity.

Totally sealing the cell without introducing friction/stiction would be impossible, although shielding the opto set up from stray light and knocks is possible but only at the expense of size.

3.4.2 Twin diaphragms

Circular diaphragms combine good linearity for small deflections, with unrivalled off axis stiffness. When operating as a parallel pair, excellent resistance to bending moments is also inherent. The layout is rotationally symmetric about the deflection axis so extra members to combat crosstalk are not required.

If the central column is designed to house the opto components at the rotational centre of the two diaphragms, the system will be very compact, with even greater crosstalk immunity.

The unit now fully encloses the sensitive optical components with no need for extra components.

However, the part count is rising. The casing and one diaphragm can be machined as one, but the central column, rear diaphragm and associated clamping system have to be separate, accurately machined components. Many close tolerance machining operations would be involved, and

assembly more complicated, leading to a sharp rise in unit cost.

The potential advantages of the set up seemed to out weigh this penalty, so the twin diaphragm layout was chosen for the initial design study.

3.5 Thermal Drift Considerations

The main enemy of many transducers is temperature related drift of sensitivity and zero point. With the very small deflections envisaged for the projected optical loadcell, minimisation of this effect was deemed to be of prime importance. To this end careful consideration was made to try and reduce potential sources of mechanical drift at the initial design stage. The loadcell body and all related components would be made from the same material, preferably the same piece of bar stock. The use of dissimilar materials and glue joints would be kept to an absolute minimum.

This source of error did indeed prove to be the major headache during the prototype development phase, specific problems and their solutions are discussed later in the relevant sections.

3.6 Design Evolution

The design process had the following main objectives:

- The unit was to be as small as possible. A loose target for overall dimension was set as follows. Case outer dimensions: 25x25x40mm.

- All possible precautions were to be taken to reduce crosstalk from off axis loads and bending moments.

- The unit must be as rugged as possible, with a large factor of safety on overload capacity.

- The unit should be cheap and easy to manufacture and assemble.

- Finally, the central column should be left as unweakened as possible to prevent distortion under load.

Initial calculations on diaphragm dimensions were carried out using formulae from Theory of Plates & Shells [7] and Roark and Young [8]. Deflections assumed that the target stiffness could be met and that the loadcell was made from EN56 free cutting stainless steel. These calculations showed up some important results.

For diaphragms of representative diameters thicknesses in the region of 0.6mm would be required, this is a realistic thickness to machine from bar stock. Roark and Young indicates that for circular plates, deflection is linearly related to load for deflection/thickness ratios less than 1/50. The estimated ratio for the loadcell diaphragms was approximately 1/250.

The maximum stress at this deflection works out to be approximately 25 MN/mm^2. This gives a load factor of safety of over 25. As discussed earlier, conventional stiff

loadcells have typical overload capacities of between 1.5 and 2. A further advantage of the low operating stress is that the diaphragms are operating well within the material's endurance limit, so fatigue should not be a problem.

All designs constrained the gratings to be at the centre of rotation of the two diaphragms, and were drawn up by first drawing the opto/grating set up, then filling in the central column and outer casing. Machining methods were considered at all stages and several proposed layouts were rejected for this reason alone.

A major area of work during the design phase was how to ensure that the gratings and optical components were accurately aligned in the loadcell. Without a high degree of alignment the loadcell performance would be degraded.

Two choices presented themselves: The grating/opto unit could be preassembled and aligned before fixing in to the loadcell body. Alternatively, provision could be made for aligning the components once they had been installed in the casing.

With space at a premium inside the loadcell body it was originally deemed to be better to set up the components in a preassembled block. This was partly due to the intention to use the Isocom dual slotted opto unit which would allow the simple scheme shown in Figure 3.2. The unit would be bonded together in a jig. The second grating would then be aligned electronically before bonding and trimming.

The Isocom dual slotted-opto unit was used in the ESPRIT project. The unit is small, can be readily split in two, has a good simple lead array and square, flat surfaces for bonding. An added advantage was that the unit was a known quantity on the project, and had already been thoroughly evaluated.

However, when it became clear that the use of gratings printed on film would be unsatisfactory, it was decided to look at what miniature discrete components were available to offset the increased grating thickness.

Designs using various combinations of discrete opto devices were evaluated, several are shown in Figure 3.2.

The pre-assembled block approach to alignment started to become less attractive when the Isocom unit fell from favour. The fact that the block was well aligned before it is bonded into the body of the loadcell could not be taken as a guarantee that it would stay aligned during assembly or in the long term. The small intricate blocks required to mount the discrete opto devices would be difficult to manufacture and did not reduce the overall size as much as expected. This led to a study of alternative methods for mounting and aligning the optical components.

Alignment of the optical system after installation in the loadcell initially seemed like a difficult task. As mentioned before, access inside the loadcell will be severely restricted. If however, adjustment can be limited to ensuring the gratings lines are parallel and setting the grating clearance, the simple system shown schematically in Figure 3.3 will suffice.

If one side of the system is mounted on a pivot pin with its axis normal to the plane of the gratings, angle and clearance are both independently adjustable. This system will only work if it is ensured that the gratings are coplanar. This should not be a problem and could be achieved to sufficient accuracy by careful bonding of the components during assembly.

There is a choice of which part of the system to mount on the pivot.

(i) The opto components with one grating,
(ii) The reference grating,
(iii) One complete half of the opto set up.

The pin would be running in a bearing in the main casing and would thus be carrying the 'fixed' part of the system. The central column carries the moving parts.

It was originally considered desirable that the opto devices should be fixed to the outer casing, to prevent movement causing changes in lead position introducing DC errors. However, this effect was deemed to be insignificant in the end because of the tiny displacements and thin wires.

The final preferred solution was to mount the reference grating on the pivot pin. This is the most space efficient solution as no clearance all round the opto set is required. The pivot pin can have a longer bearing length aiding alignment. The overall casing size and access port diameter can be smaller due to the reduced size of the pivot block and simpler lead routing. Schematic cross-sections of the two options are shown at the same scale in Figure 3.4.

This arrangement was studied for several different opto pairs to try and find the most compact arrangement.

The smallest devices found were the Honeywell SD#/SE# matched pair. These had an incredibly small package size and seemed to have good optical characteristics. Various layouts were studied to accommodate these units. However due to their contact configuration they proved difficult to mount. The rear portion of the package is a metal can that forms the cathode, this must be electrically isolated from

the case, leading to an unacceptable increase in package size and manufacturing complexity.

The most satisfactory layout seemed to be with side viewing components. This configuration allows all the component leads to emerge in a single direction, as with the Isocom slotted unit. Unfortunately the majority of infrared devices proved to be in-line viewing. No dedicated opto pairs with this layout were commonly available.

The Farnell catalogue has a large range of optos and a workable combination was found in the form of a Honeywell SEP series emitter and the Telefunken BWP41N PIN photodiode. These two are not spectrally matched, and the half intensity angle of the emitter is 50 degrees. This means that collimation would be poor. However, the peak sensitivity wavelength of the PIN diode was none the less close to the peak irradiance frequency and the large area of the receiving diode should lead to reasonable output even with poor collimation.

It was decided that this combination was the most promising with all factors including size, cost and performance taken into account.

On examination the BPW41N package appeared to be larger than necessary. One was sacrificed and the plastic casing melted away to examine the internal layout of the unit. It was found that a large proportion of the package could be removed. The only constraint was a very fine wire linking the cathode to the external lead. This projects upward approximately 0.8mm into the case (See Figure 3.5).

The BPW41N's were trimmed accordingly, resulting in a very thin package. The machined front and rear faces proved ideal for mounting purposes.

3.8 Basic schematic design

At this stage a full initial design was drawn up for general appraisal. This was to form the basis for the first prototype and as such is discussed in detail in later chapters. However, a brief outline is included here in order to give insight into the design of the testblock described in the next chapter.

The first complete design was a marrying of the various factors discussed in preceding sections. The layout was similar to that shown in cross section in Figure 3.4(b). The unit was designed around the side-looking emitter and PIN diodes described above. The optical components, and one grating, were housed in a pocket in a central column linking a pair of diaphragms at either end of a square casing. The second grating was mounted on a pivot pin as described earlier. Lead exit was via a multi-pole Lemo style connector.

A low-rate biasing spring was included behind the rear diaphragm to allow the output to be zeroed after alignment

These themes were to be developed as a result of experience gained from the optical system evaluation trials.

3.9 Conditioning Circuitry

The conditioning circuitry would also play a large part in making the system viable. The signal noise voltage will in the end determine the resolution of the system. Part of the noise is generated by the active and passive components in the conditioning circuits. Thus the electronics have to be treated as a noise critical application and components selected accordingly.

The conditioning circuitry can either be sited locally or remote from the loadcell unit, or a mix of the two.

Local siting reduces problems with noise pick up and piezo noise generation from long cables and potentially reduces the number of wires. However, anything other than very basic conditioning starts to take up significant space. The compact nature of the loadcell would be compromised.

As long as cable lengths were kept reasonably short and twisted pair cores with overall shielding are used for the critical signals, noise pick up should be minimal. The photodiode generates a photocurrent not a voltage, so other problems usually associated with small signal transmission, such as resistive voltage drops, are not a problem.

The mixed approach is probably the most attractive proposition if the loadcell were to be put into production. Fabrication of a dedicated receiver I.C. incorporating the photodiodes and initial conditioning would be cheap for a large production run, and would reduce size overcoming the main objection to insitu conditioning.

3.9.1 Photodiode Conditioning.

The are various modes in which a photodiode can be used. These are the photovoltaic mode, photoconductive mode, and the photoamperic mode.

The photovoltaic mode is not useful because the output is a logarithmic function of light intensity.

If the photocurrent of a reverse biased photodiode is fed to ground through a high value of load resistance the result is a system with a linear relationship between incident light and output voltage. However, a photodiode

operating in this mode generates more noise because leakage current increases with back bias.

The most useful configuration for this application is the photoamperic mode. Here the photodiode is connected to a low value of load resistance. The output current is linearly related to incident light.

The usual method of providing a low load resistance is to connect the diode to the virtual earth of an operational amplifier. A large value of feedback resistor is then chosen to convert the small photocurrent, typically a few microamps, into a useable signal voltage. The opamp has to be chosen carefully to combine a very low input offset current with low output noise and high power supply rejection characteristics.

The opamp chosen for the job was the Burr-Brown OPA121KP. Full performance and application details can be found in the manufacturers data sheets.

3.9.2 Emitter Drive

The simplest drive scheme is a constant current drive. This would have to use some form of active current source if noise and drift levels are to be acceptable. A programmable current source such as a National Semiconductor LM334Z or an opamp configured as a power amplifier would be used.

Infrared components generally have fairly poor temperature coefficients. The irradiance of the emitters would directly effect the amplitude of the output signal. Thus if a simple constant-current emitter drive system was adopted the temperature stability of the loadcell would be poor.

A more satisfactory scheme would be to control the emitter drive current using the summed output from the two receivers. This means that the output from the photodiodes is dependent only on the temperature coefficient of the voltage reference used in the control loop. This would greatly reduce temperature drift problems. This approach was suggested by Tom Stevenson.

Long term drift would also be reduced to circuit component values. Degradation of the gratings and long term drift in the properties of the optos themselves would be largely self compensating.

The critical element in such a system, as indicated above, is the voltage reference used in the error amp. The reference needs to be adjustable to allow the circuit output to be stabilised and optimised. The output noise must be as low as possible. Finally, and most importantly, the temperature coefficient must be minimal. The National Semiconductor LM317LZ programmable voltage regulator proved to be ideal. The reference voltage is set using two external resistors. The output is filtered using capacitors from the output to ground across a load resistor. Full performance figures and application notes can once again be found in the manufacturers data sheets.

Once the required output voltage had been set using an external resistor value switch box, the chosen value would be soldered in.

3.9.3 Output Conditioning

As explained earlier the two opto outputs are phase shifted by 180 degrees. The two signals would be passed through a differential amplifier to give the required "push/pull" output. This output can be heavily filtered as it is outside the emitter drive feedback loop.

3.9.4 General Minimisation of Noise

The usual general rules for minimising noise generation and pick up within the system apply.

Any small signals are immediately amplified up to large voltages to make component noise contribution only significant in the initial stage.

Power supply rails must be well bypassed using both electrolytic and ceramic capacitors to cope with all frequencies.

All vulnerable components should be shielded. For the prototype this would be compromised to allow easy routine access to test points and trimmer potentiometers.

The components themselves contribute to the noise and so have been chosen carefully. Generally the more components and stages, the greater the build up of white noise. The prototype circuit would incorporate many components that would become redundant and so should give a pessimistic estimate of background noise levels.

DC drift also is a form of noise. The main cause of drift in electronic circuits is temperature. Drift due to ambient temperature fluctuations cannot be avoided. It can be minimised by appropriate choice of components. All resistors should be at least metal film 1% specification. These have temperature coefficients of less than 100ppm/C. Circuit board layout also has an important part to play. Many of the circuit elements generate a fair amount of heat themselves. If these components are not sited carefully, they may cause larger drift problems. In the circuit layout chosen, the emitter current driver, a 5534N, is kept well clear of the critical OPA121 photodiode conditioners.

The differential nature of the final conditioning removes most of the coherent noise on the two photodiode outputs. The noise remaining is mainly broadband 'white' noise, much of this can be removed using a low pass filter on the differential stage. The roll off frequency of this filter is the measurement bandwidth limit of the loadcell.

3.10 Conclusions

A detailed feasibility study was carried out of all components of a loadcell using optical deflection measurement.

A further study evaluating various conditioning electronics options was also carried out.

Provisional designs were drawn up from the findings.

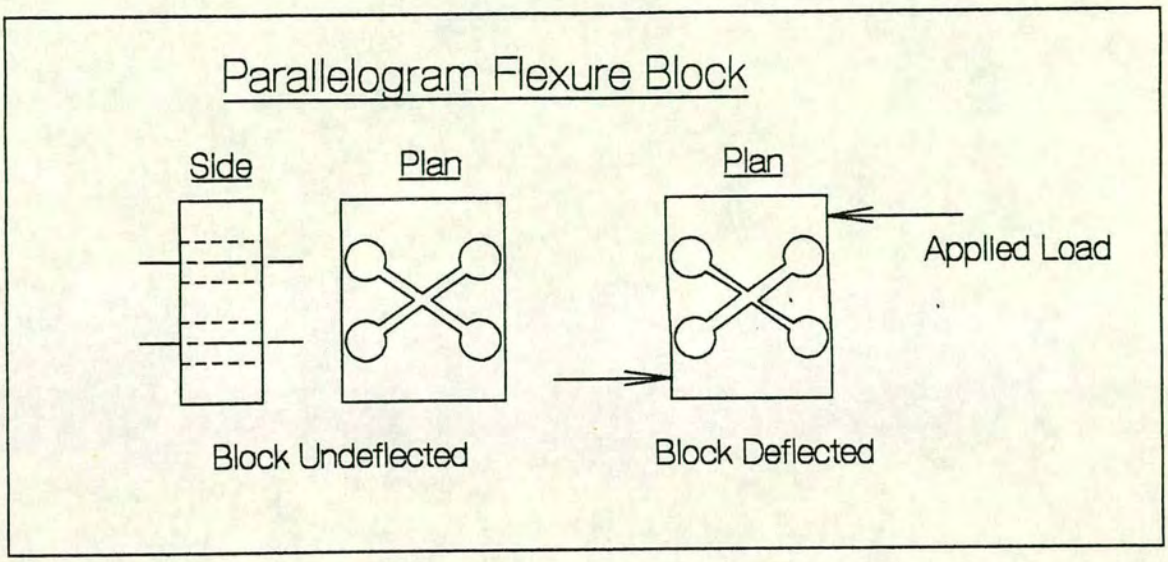

Figure 3.1 Parallelogram Spring System

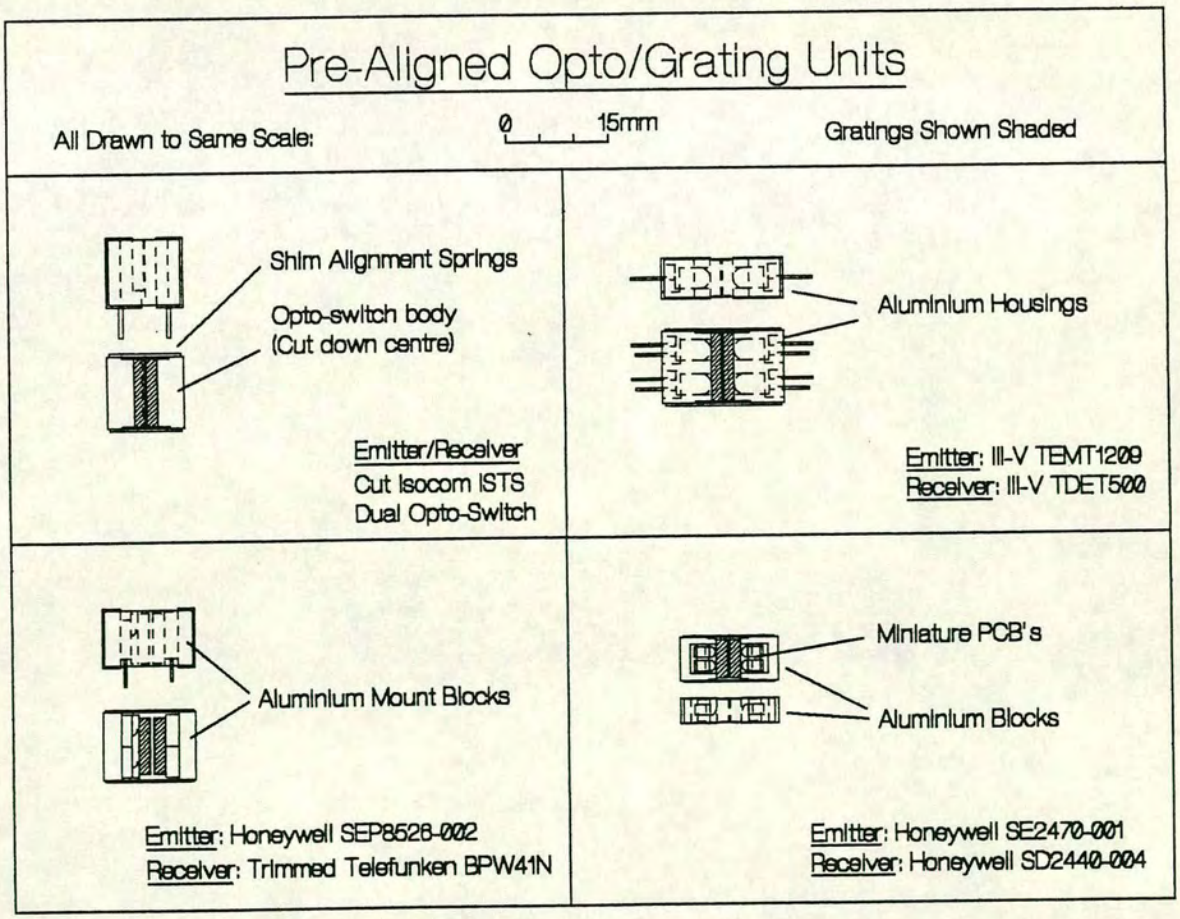

Figure 3.2 Pre-Aligned Opto/Grating Units

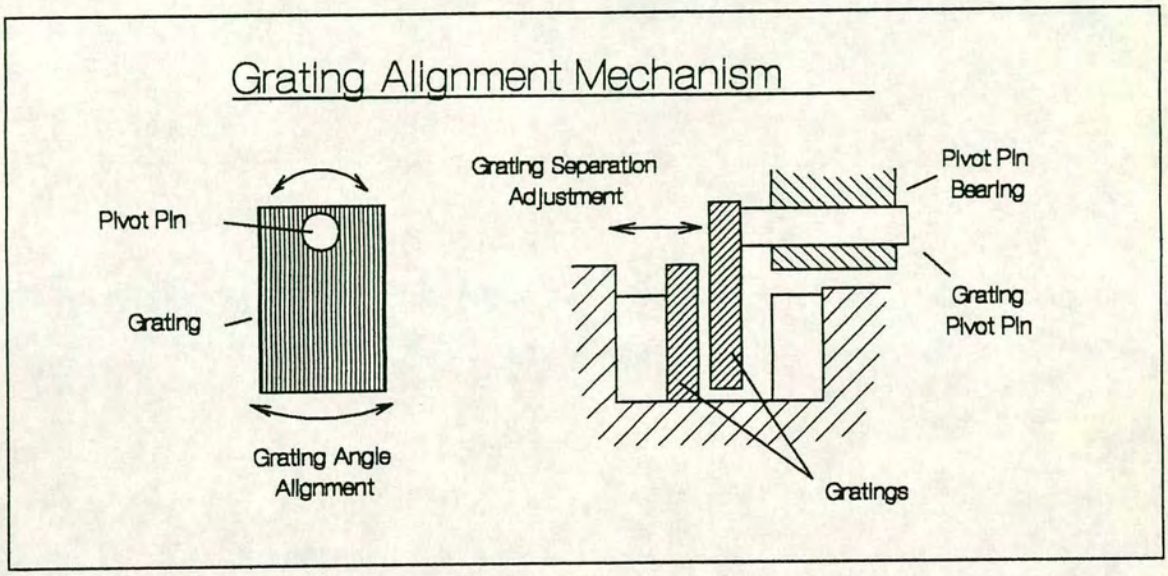

Figure 3.3 Grating Alignment Mechanism

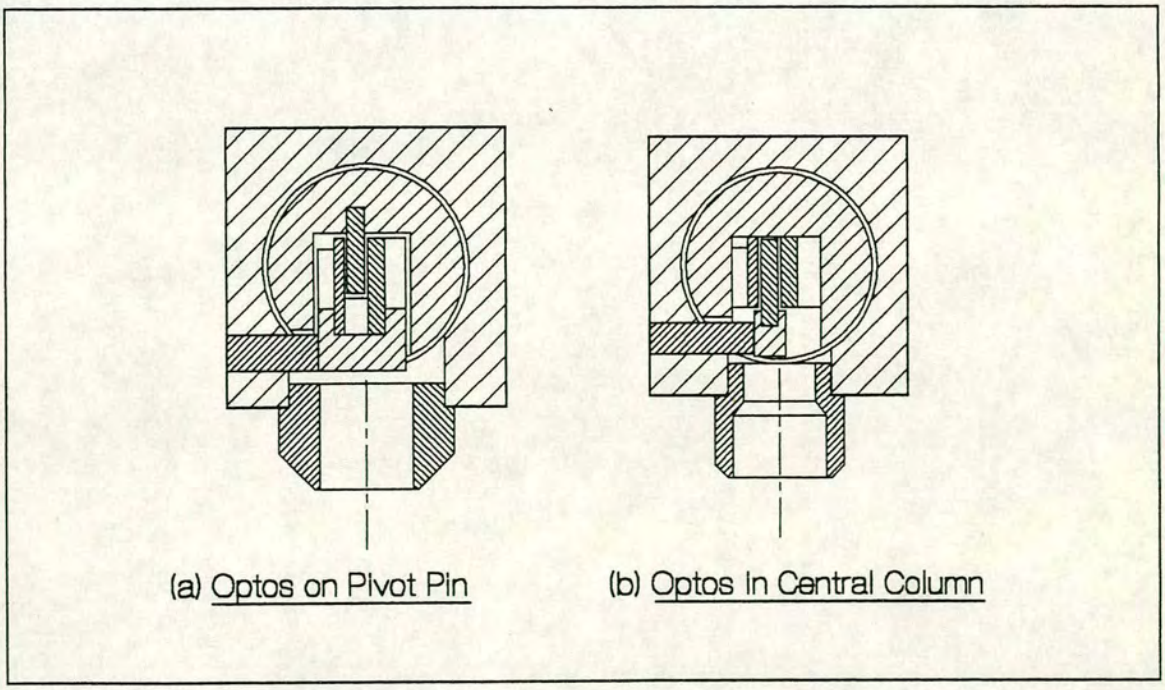

Figure 3.4 Choice of Opto/Grating Mounting

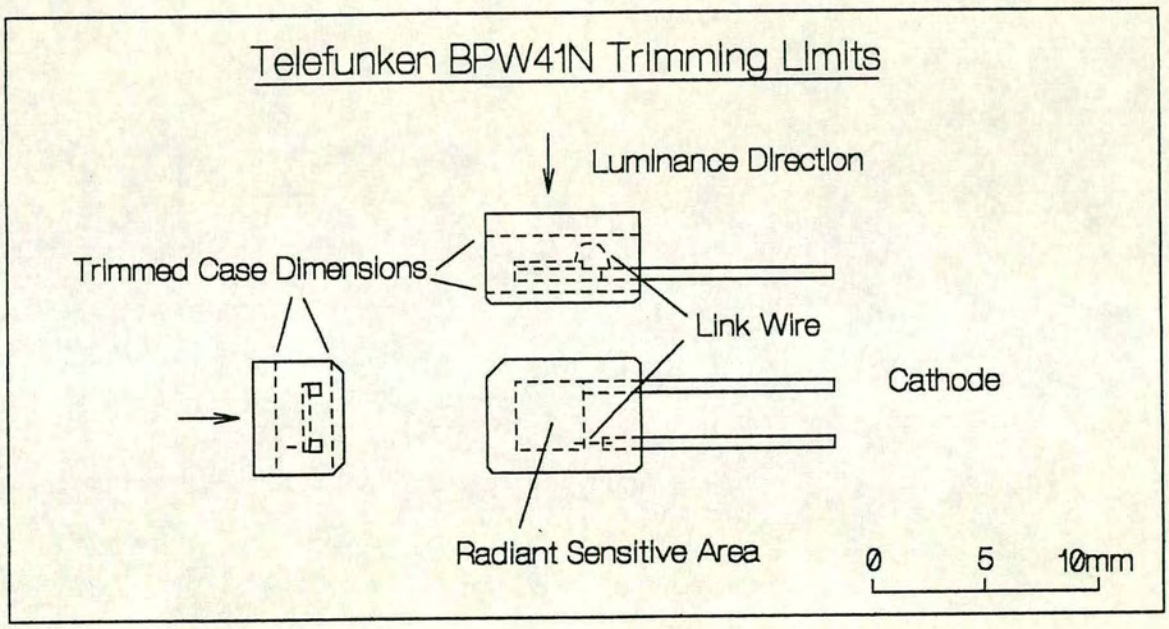

Figure 3.5 Telefunken BPW41N Internal Layout

Chapter 4. Testing the Optical System

4.0 Chapter Summary

This chapter presents results and findings of an experimental investigation of the optical system. Problems encountered during testing and their solutions are described.

Tests using various optical components and grating pitches are discussed, and estimates of loadcell performance predicted for each configuration.

The chapter concludes with a discussion of the influence of the test programme on the design of the initial, and subsequent prototypes.

4.1 Testing of the Optical System

The optical system is the heart of the new loadcell. All aspects of the system had to be thoroughly investigated to isolate problem areas, develop strengths and assess its potential.

The real unit is designed to be as compact as possible. Thus, space is at a premium and access limited, making testing, observation and alterations through the test series difficult.

To ease the job of system evaluation a more open testblock was designed and built. It incorporates all the important features of the real unit, but has a simpler, open parallelogram spring system, machined from the solid block. This spring scheme was to introduce problems of its own, but overall the testblock proved to be an excellent evaluation tool. Changes of grating,optos and other modifications were quick and simple, and a lot of visual checks of alignment and possible problems/conflictions were possible.

The grating separation, d, and alignment angle, theta, are variable in exactly the same manner as the real unit. The pivot pin was significantly longer than the full design, this again introduced problems, but gave a worst case limit for pin slop/play.

The gratings are deflected across the test range by a low rate spring driven by a set screw tapped into the fixed part of the testblock. This spring was changed throughout the test series to give the most sensitive adjustment, while still giving adequate reserve throw. Deflection of the block was measured using a precision L.V.D.T. made by Tessa. This is designed to be used for component dimensional quality control and has a maximum resolution of 30nm.

The underside of the deflecting portion of the block is relieved to prevent drag on the mounting surface.

The whole block was black anodised to reduce reflections within the pocket.

The unit was designed to carry out tests on sensitivity, linearity, full scale range and the effects of grating separation and theta misalignment for the various different grating pitches. To allow the optos and gratings to be changed easily, the components were bonded in with only a minimal amount of low strength retainer. The reference grating however was bonded in more securely, as contact with the moving parts could have, and did in one case, result in movement and thus false results.

Figure 4.1 shows various views of the testblock, with all important features annotated or expanded.

4.2 Set up of the Testblock

To ensure alignment of the various components of the testing system, the parts were assembled on a small ground surface table. Collinearity is ensured using a workshop parallel. The Tessa LVDT probe was mounted in a pinch block with the bore machined accurately to the reference face which rests against the parallel.

Two separate micrometers were used to vary the grating clearance, d, and the relative grating angle, theta. The grating clearance micrometer was a 0-25mm open ended height gauge to ensure good alignment, allowing the grating clearance to be set to within 0.005mm. Theta was controlled by a 0-25mm digital read-out micrometer via a torque-arm. A polished ballbearing is bonded to the end of the arm to ensure that the adjustments are as linear as possible over the test range. The length chosen allows the micrometer to be read directly to 0.001 degrees.

Initially all the components were clamped magnetically, however different clamping methods were adopted as the tests progressed as described later.

A prototype circuit was built using the ideas discussed in Section 3.9. Several features were included to allow easy setting up and modification. It was accepted that these may compromise the performance to a certain extent. A full circuit diagram is shown in Figure 4.2.

The circuit sat alongside the surface table and was unboxed to allow easy access to testpoints and trimmer potentiometers.

Measurement of signal noise presents a problem. The inherent noise of many measuring instruments is of the same order as that on the opto circuit output. Accurate estimation is only possible if the noise component of the

signal is amplified. An A.C. coupled 0.1Hz - 1.2kHz amplifier with a gain of 100 was built to examine the noise on various voltages around the loadcell conditioning circuit. The circuit output noise was estimated to be 1.5mV R.M.S.

Initial tests were carried out using an oscilloscope to determine voltage ranges and polarities before connection to the sampling system.

4.3 Initial BBC Computer Testing System

David Jeffery had set up a sampling and analysis system using a BBC Micro to evaluate the opto-gap sensors used in the Esprit Project. The facilities available were broadly in line with my requirements so I decided to adopt this option. The LVDT and opto outputs were connected to the BBC Analogue port via a small interface card, which scales and offsets the input voltages. The system was recalibrated using a precision DC reference supply and several new program routines were written to cope with the different specific requirements.

The LVDT voltage range is subdivided into 20 equal boxes. The program samples the two channels until it has three values in each box, ensuring a reasonable spread of values over the whole range. A graph of opto output v's displacement is then plotted and several key statistics calculated and displayed. These include: the peak to peak range, the maximum gradient and linearity estimates for the test. These routines were modified to cope with the new set up. A new file handling routine was written that saved the tests automatically as a numbered series with a global header.

Initial tests with this set up proved to be very promising. The graphs were smooth considering the sparse data points and sensitivity, peak to peak range and linearity were all along with expectations. However when the results of a test series sweeping through a range of values of theta were plotted several anomalies were discovered that suggested that something was amiss in the system. The values obtained from the program were not repeatable.

A large amount of extra software would have had to be written to allow detailed analysis and comparison of test results. The initial results were positive enough to warrant further investigation so alternatives were looked for.

The PC based sampling system at the Wide Tank was one option considered. A wide range of sampling and data handling routines are available, but all the analysis software would have to be specially written.

During the ESPRIT Project David Jeffery and Jon Muhl, Edinburgh University Wavepower Project, had set up powerful PC based data acquisition and analysis package using the GFS DIA software and Microlink sampling hardware. This system had been thoroughly tested and seemed to be ideal for the job.

4.4 Set up with PC/Microlink/GFS DIA

The Microlink sampling box is a modular 19" rack based sampling system with its own clock, buffer memory and analogue-to-digital converter. Communication with the host PC is via a GPIB interface. A set of home-built 15Hz 2nd order anti-aliasing filters are mounted in the rack and were used for all testing except where indicated.

The GFS DIA software is a commercial data analysis package, incorporating a macro programming language to allow control of the sampling hardware via the GPIB interface. Full analysis tools are available including; graphical, statistical, spectral and mathematical. David Jeffery had written a general purpose sampling and data storage macro that proved to be suitable with only a few minor modifications.

The maximum input range of the Microlink is 10 Volts. This can either be used as a unipolar range, or can be divided up using the offset trim to give bipolar ranges. The box was set up to have bipolar inputs of +-5V. The peak output from the opto conditioning circuitry is around +-7.5V, so an interface circuit with a gain of 0.5 was built. The LVDT output is +-1V so can be connected to the Microlink directly.

The system was again recalibrated using the reference source. All calibration procedures related input voltage to computer binary output directly to avoid cumulative calibration errors.

Figure 4.3 shows a schematic of the testing system.

For most of the tests the Microlink was set up to sample at 20Hz for 20 seconds. This was sufficient time to allow the gratings to be moved smoothly across the test range.

Initial tests with DIA gave much smoother graphs due to the greater number of data points and the more stable, lower noise sampling system.

The repeatability problems hinted at by the BBC results showed up clearly when several tests were plotted on the same axes. The power and versatility of the Microlink/DIA combination proved to be invaluable in tracking down the various sources of error.

4.5 Improving Repeatability

The repeatability problems were systematically identified using various experiments to highlight the effect. The problems that could be solved were dealt with, problems inherent in the design of the testblock were allowed for in the results.

The following problems had to be traced and solved:

Initial results showed that the tests showed a reasonable degree of repeatability as far as peak/peak range and slope were concerned. However, the graphs seemed to fall in a spread along the X-axis (see Figure 4.4). This was traced to movement of the testblock between runs. The testblock and LVDT mount block were subsequently held in place with a small drop of retaining compound in addition to the magnets.

Similarly, the two micrometers were found to be susceptible to movement during a test series. The micrometer controlling the grating separation was holding well on a magnet but the magnet was pivoting easily on the parallel. Again a small drop on retainer cured this. The theta micrometer was adjusted continuously, the barrel was exposed to accidental knocks leading to misalignment. A mounting block incorporating a mechanical clamp was built to prevent movement.

The grating pivot pin in the real loadcell would be very short. This means that slop between the alignment bore and pin should have little effect on the output. As explained earlier, the geometry of the testblock necessitates the use of a substantially longer pivot pin. Observed humps and hollows on the test curves, and the general low repeatability of the system were attributed to this.

The use of kilopoise grease on the pivot pin improved the results but it was deemed that a new pivot pin was required.

A new, thicker pivot pin was made from 6mm diameter ground stock stainless steel. This pin was offered up to various reamed test holes to find the optimum combination. A nominal working clearance of 0.005mm was found to be adequate when used in conjunction with the Kilopoise grease.

With the pivot in this final guise the system repeatability increased to acceptable levels, even after fairly rough disturbances to the test block. Figure 4.5 shows 5 tests plotted together. The tests are all at the same grating clearance and theta angle. However, each time the theta micrometer was backed off to a different position and the pivot pin wobbled by hand, before returning the gratings to their original angle. The peak/peak range is repeatable to +-0.2%, while the gradient of the central portion of the test curve is repeatable to within +-0.4%. These were deemed to be small enough repeatability bounds to carry out a reasonable test series.

The lower accuracy of the gradient is almost certainly due to bandwidth limitations of the Tessa LVDT. The probe/conditioner combination is really designed for D.C. applications such as dimensional quality control. The output signal is heavily filtered to reduce noise, severely restricting the available bandwidth. This means that if the motion of the testblock is at all jerky, the inherent damping in the Tessa system causes a phase error which appears as a glitch on the test curve. Although small this has a disproportionately large effect on the regression coefficients. The peak/peak range is unaffected as this is not dependent on the LVDT output.

A couple of bandwidth test were carried out to illustrate this effect.

Figure 4.6 shows the output from the opto set and LVDT while the testblock was being deflected vigorously. The LVDT trace lags the opto readout even at this low frequency (approximately 7Hz). The steps on the traces are quantisation errors due to the small voltage amplitudes.

Figure 4.7 shows the output from the two transducers with the test block resonating freely (approximately 600Hz). The opto output seems to be following the exponential decay nicely. The LVDT however is well outside its bandwidth. The heavily filtered output is compounded by mechanical damping in the probe. The LVDT head obviously loses contact with the testblock. As the probe reestablishes contact, the opto output signal shows a re-excitement of the testblock resonance.

Due to the parallelogram configuration of the testblock, the grating clearance reduces as deflection increases. This was originally assumed to be insignificant. However, general rising or falling trends, and/or steps in the results were traced to this effect.

Finally, it was observed that the plots of opto output v's displacement showed a visible asymmetry, one end being more rounded than the other (Figure 4.4). Examination of the individual opto outputs showed a similar shape, with the two curves offset from each other.

This effect could be due to a number of things including; differences in emitter irradiance, differences in receiver sensitivity, or shuttering asymmetry. The emitter drive voltage was examined to see if its behaviour would give any clues to the reason for the system asymmetry. Figure 4.8 shows the opto-output over 2 complete cycles. Figure 4.9 shows the corresponding emitter drive signal. Figure 4.10

shows the individual opto outputs for a similar test set up.

These tests led to suspicions that the latter, shuttering asymmetry, was the cause of the problem. This was because; Opto 1 has a very low 'dark' output even though overall emitter intensity is rising while the output of opto 2 does not drop to a very low level even though as the gratings close the overall emitter drive demand is falling.

To find out if this was the case, the feedback loop was broken and the emitters were driven by a current limiting bench power supply. If the supposition that it was some form of shuttering asymmetry that was causing the problem was correct, it would be expected that with a constant current drive, the individual opto outputs would have different peak/peak ranges and gradients, but similar zero offsets. Each graph would exhibit similar (symmetrical) end effects.

If however it was an opto device imbalance that was responsible for the phenomenon then similar gains and ranges would be exhibited by the two pairs, only the zero offset would be different. The asymmetrical ends in this case would be due to the exact phasing of the peaks and troughs of the two opto pairs.

Figure 4.11 shows beyond reasonable doubt that the asymmetry is due to a grating misalignment. The individual curves are self symmetric, but far from mutually symmetric. Opto 1 shows, as expected, a much steeper curve with much more efficient shuttering that Opto 2. The zero offsets of the two curves are similar now the unbalancing effect of the closed loop emitter drive has been removed. The visible noise on the traces is output supply ripple from the bench power supply.

On very close inspection the gratings proved to be slightly misaligned when viewed from above (see sketch, Figure 4.12). The degree of misalignment can be estimated from Figure 4.11 and appears to be around 0.025mm.

With the feedback loop re-closed a final check was carried out with a large grating clearance to see if symmetry improved. The results in Figure 4.13, show a good improvement in symmetry as the grating clearance becomes large relative to the misalignment.

4.6 Tests using Original Opto's

With the system repeatability problems solved several test series were carried out to evaluate the optical system.

These tests were designed to determine:

- Maximum resolution
- Sensitivity to grating alignment (theta)
- Sensitivity to grating separationd (d)

for the various grating pitches available.

As explained earlier theta and d could be varied independently with workshop micrometers. Initial sweeps were carried out to determine suitable measuring ranges. The best format for the test series was deemed to be sweeps of theta at various grating separations.

4.6.1 10 lines/mm Gratings

The results from the various sweeps for the 10 lines/mm gratings are shown in Figure 4.14 and Figure 4.15.

The large step/discontinuity in the curves is due to the parallelogram effect outlined earlier. It was decided that in order to prevent too large a systematic error creeping in the gratings would be stepped at intervals, instead of following the same line pairs across the test range. This will reduce the chance of mislocating and overestimating the peak.

The results show that the system is very sensitive to grating clearance but insensitive to theta misalignment.

The sensitivity to grating clearance is due to the poor collimation of the optical system. With gratings of this pitch diffraction is not a problem [5]. Diffraction effects do not become significant until gratings of more than 25 /mm are used, and are not dominant for gratings of less than 50 /mm.

The insensitivity to theta errors was more of a surprise. The p/p output and maximum gradient are virtually unaffected over a range of +-0.1 degrees and remain within 2% of the maximum values over a range of +-0.25 degrees. This yields important benefits as explained later.

The tests results in conjunction with the signal noise figure give a estimate of system potential. The optical system in this configuration allowed a peak resolution of 3.7nanometres. Although this did not meet the target of 2.5nm the results were none the less encouraging.

Figure 4.16 shows the test traces for theta=0 at the three grating separations.

4.6.2 25 lines/mm Gratings

The testblock was then fitted with gratings with 25 lines/mm. An initial set of tests was carried out using experience gained from the first set.

Results continued to be promising but the fall off of performance as 'd' increased was very marked as seen in Figure 4.17. This is because diffraction effects are starting to cause significant degradation of shuttering efficiency in addition to the collimation problems. This would necessitate a working clearance of less than 0.05mm which, it was deemed, would be difficult to achieve.

An improved peak sensitivity of 0.65 V/um was noted. The output noise was the same as before giving the new system a resolution of 2.5nm. This met the target resolution for a loadcell with a full scale deflection of 2.5microns. However, as explained above very small grating clearances were required to achieve these figures.

4.7 Tests using New Opto's

While these initial experiments were being conducted a continued search for better opto components led to a new range of side-looking opto pairs. These had far better collimation performance than the original set. The packages are also smaller in all but thickness allowing the use of a narrower and shallower opto pocket.

The receiver is a phototransistor rather than a PIN photodiode. These have a lower bandwidth, however with typical rise times of 3-4 us, this is not a problem for this application.

The conditioning circuitry needed to be modified to accept the new optos. The emitters were similar to the old ones

and so only a small change of current sensing resistor was required.

The phototransistor receivers are, unlike the old units, lensed with a narrow viewing angle. The new conditioning circuit is shown in Figure 4.18. A bias voltage of +13V was chosen for convenience, leading to typical output currents in the range of 0.5 - 1.0 mA. This means that a much smaller resistor can be used in the OPA121 conditioners. The larger output current gives the added advantage of reducing problems of using the loadcells with long connection leads, and reduces susceptibility to noise pick up.

Due to the narrow half angles of the new components, accurate alignment of the optical centres was now more critical. A convenient way of achieving this was to use an aperture plate similar to that used with the old emitters.

The circuit in its new configuration gave a 0-1kHz signal noise of 0.7mV RMS. The noise figure has reduced mainly due to less electromagnetic pick-up due to the much output higher currents generated by the phototransistors.

The current transfer ratio of the system is vastly superior which means that the emitter drive current is approximately a quarter of the old value. This means that the system will run much cooler, reducing potential drift problems and further reducing signal noise in general.

The system was configured for 25 /mm tests. A similar set of evaluation trials were carried out. Figure 4.19 shows the relationship between peak/peak voltage range and grating alignment for various grating separations. It can be seen that the better collimation of the new optos leads to a much more gradual fall off in performance as the grating separation is increased. Figure 4.20 shows the gradient of the central portion of the test curves. This

indicates peak sensitivities of better than 1V/um. This gives the system a resolution of 0.7 nanometres. Just as important as this is the fact that resolution is still approximately 1 nanometre with a grating separation of 0.05mm, and better than 3 nanometres even at a separation of 0.1mm. This reduced sensitivity to 'd' was a very important result.

Figure 4.21 shows the individual peak traces at the various grating separations. Figure 4.22 shows the individual opto outputs for these cases.

It was decided to halt development of the optical system at this point. Ample resolution had been achieved and it was expected that development of the loadcell itself would take a significant amount of time.

4.8 Influence of Tests on the Loadcell Design

The tests carried out with the testblock proved to be invaluable. Critical areas of the system were highlighted and several simplifications could be made to the design.

The sensitivity tests indicated that the target stiffness could be comfortably achieved. Indeed a full scale deflection of less than 1um should be achievable. With maximum loadcell stiffness a major aim it was decided to uprate the specification to this level for the initial prototype.

The non-optimum collimation and diffraction effects combine to mean that a very small grating clearance has to be used. The small clearances lead to an undesirable sensitivity to out of plane alignment of the gratings. However, the closed loop control of the emitter irradiance goes a long way to reducing this problem.

Several options were open to cope with the small clearances required. The alignment could be trusted to accurate manufacture and jig gluing of the optical components and gratings. The gratings could be bonded in after the unit has been assembled. The other choice, suggested by Win Rampen, is to have one of the gratings on a compliant mount, with a low friction bearing element of the desired thickness between the gratings.

Figure 4.23 shows a possible implementation. The grating must be constrained accurately against movement in the 'theta' and 'x' direction as shown, but must be free to align itself in planar orientation and clearance relative to the fixed grating. A low rate spring imparts a small closing force to maintain alignment. The PTFE film bearing element ensures a low friction/stiction bearing while ensuring a constant grating clearance.

This method of grating alignment has several advantages and drawbacks.

Good alignment of the gratings would be ensured. Crosstalk from off-axis loads and bending moments will be reduced as these will no longer affect grating alignment. The manufacturing tolerances on the main components will be relaxed, which would reduce the cost of the units.

However, the units would become much more complicated, with both the part count and assembly time rising sharply. The bearing surface would generate a significant stiction and friction, and may lead to debris generation within the unit (such as emulsion flaking). The current transfer ratio would fall because of the almost inevitable increase in separation of the opto pairs. Finally, the opto pocket itself will have to be enlarged, necessitating a larger central column and outer casing. The opto pocket would become increasingly difficult to machine accurately as it becomes deeper.

It was decided to shelve this idea unless it became absolutely necessary.

Trusting the alignment of system components to the manufacturing accuracy is a feasible method. The machining tolerances required are achievable. The extra cost of machining to this accuracy would be offset by the reduced assembly time and lower part count.

At the design stage the best compromise seemed to be gluing in some of the components after the main body of the loadcell has been assembled. The chosen method was gluing the fixed reference grating into its mount block after assembly.

The rear face of the receivers would be milled coplanar to the front face of the aperture plate before bonding to its grating and into the central column. This would ensure alignment with the deflection axis and reduce size. After assembly the fixed grating would be lightly held against the receiver grating by 'soft' spacers while a gap filling glue set.

The low sensitivity to theta misalignment means that the bias spring discussed in Section 3.8 was unnecessary. The grating pivot axis is displaced from the optical centre. This means that biassing the system onto the linear part of the output curve can be achieved by altering theta, with minimum loss of system sensitivity. This in turn increases the overload capacity of the loadcell because the diaphragms are not pre-strained more than necessary.

The problems with slop in the grating pivot could be serious, given the small pivot bearing length available. The pivot axis was moved as near to the edge of the unit as practical and the overall casing dimensions increased to maximise the available bearing length. The scheme used for the revised pivot pin in the testblock, to minimise bearing

clearance, would be adopted. After set up the pin would be rigidly clamped or bonded.

4.9 Conclusions

- An extended test series examining all aspects of the optical system was carried out.

- Several different configurations were tested.

- A system resolution of less than 1 nanometre was achieved.

- Predicted loadcell performance figures were calculated from the test results.

- Critical areas of the system were identified and recommendations for revisions to the original design were formulated.

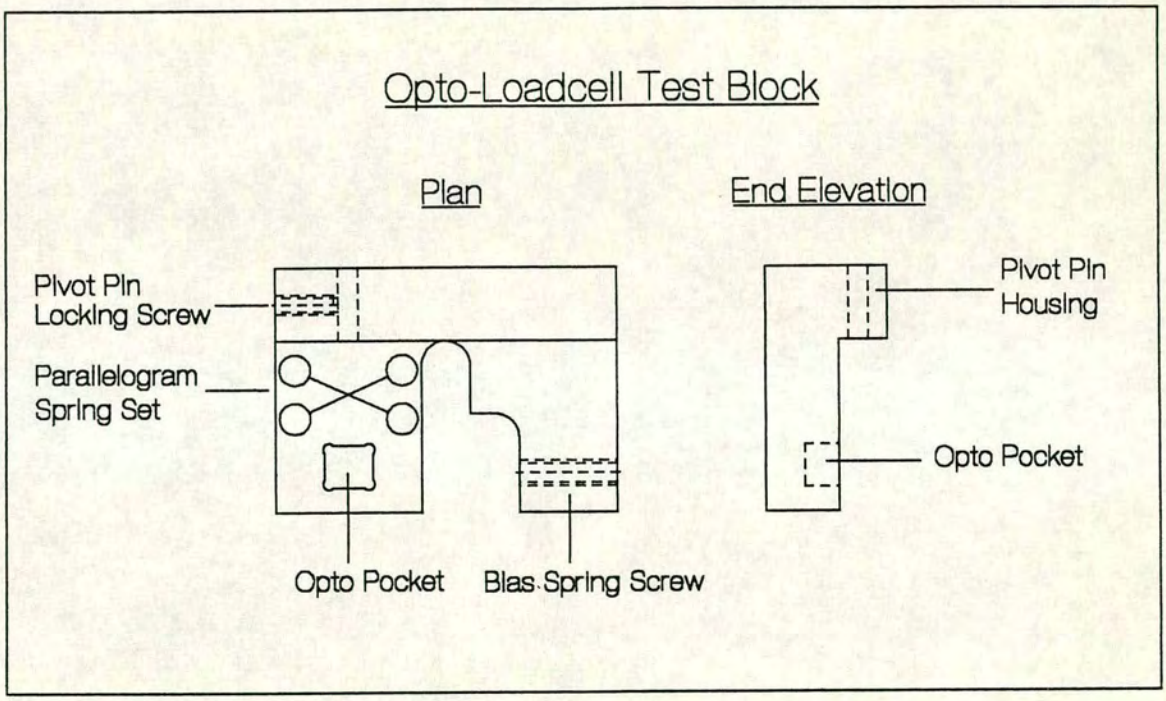

Figure 4.1 Testblock Detail

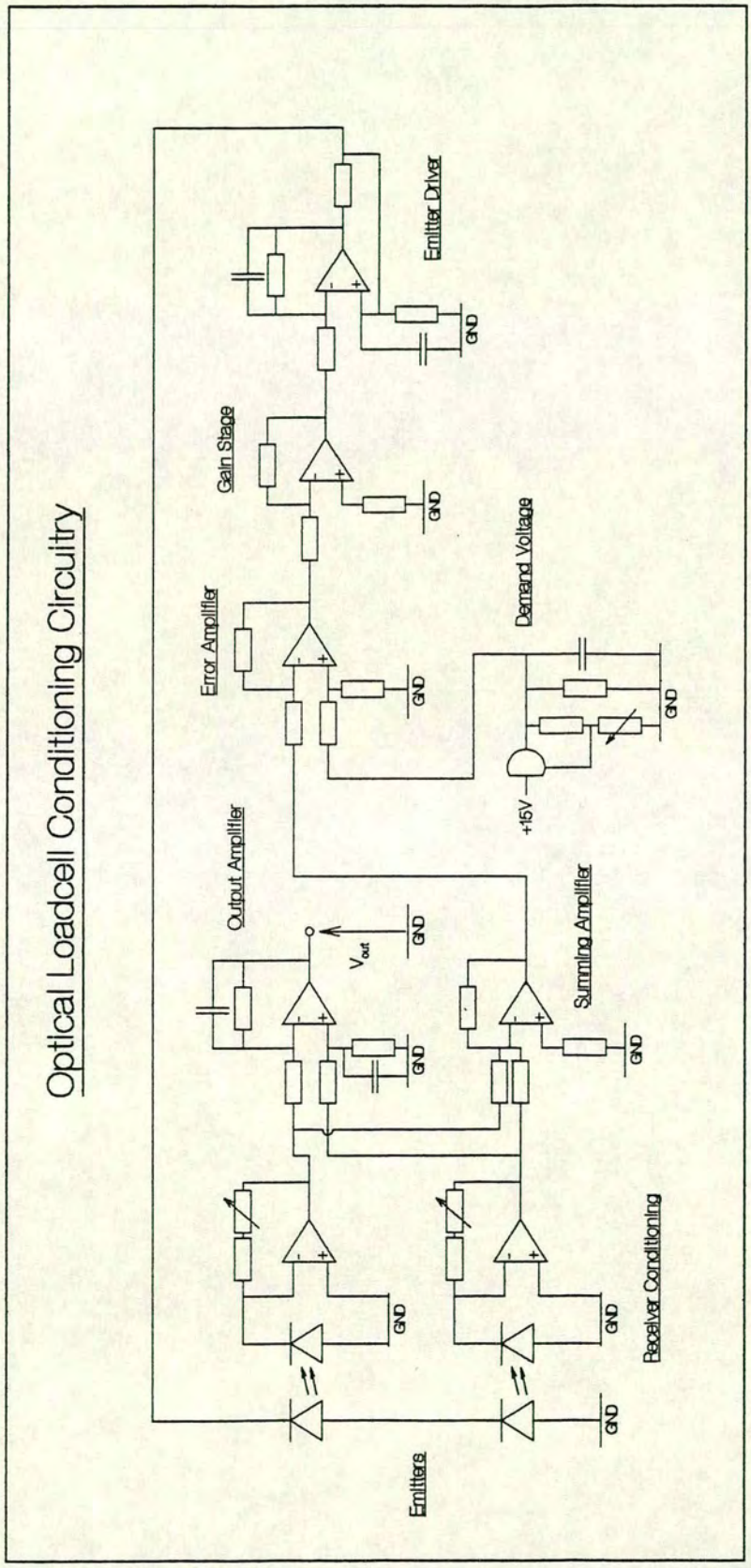

Figure 4.2 Prototype Conditioning Circuitry

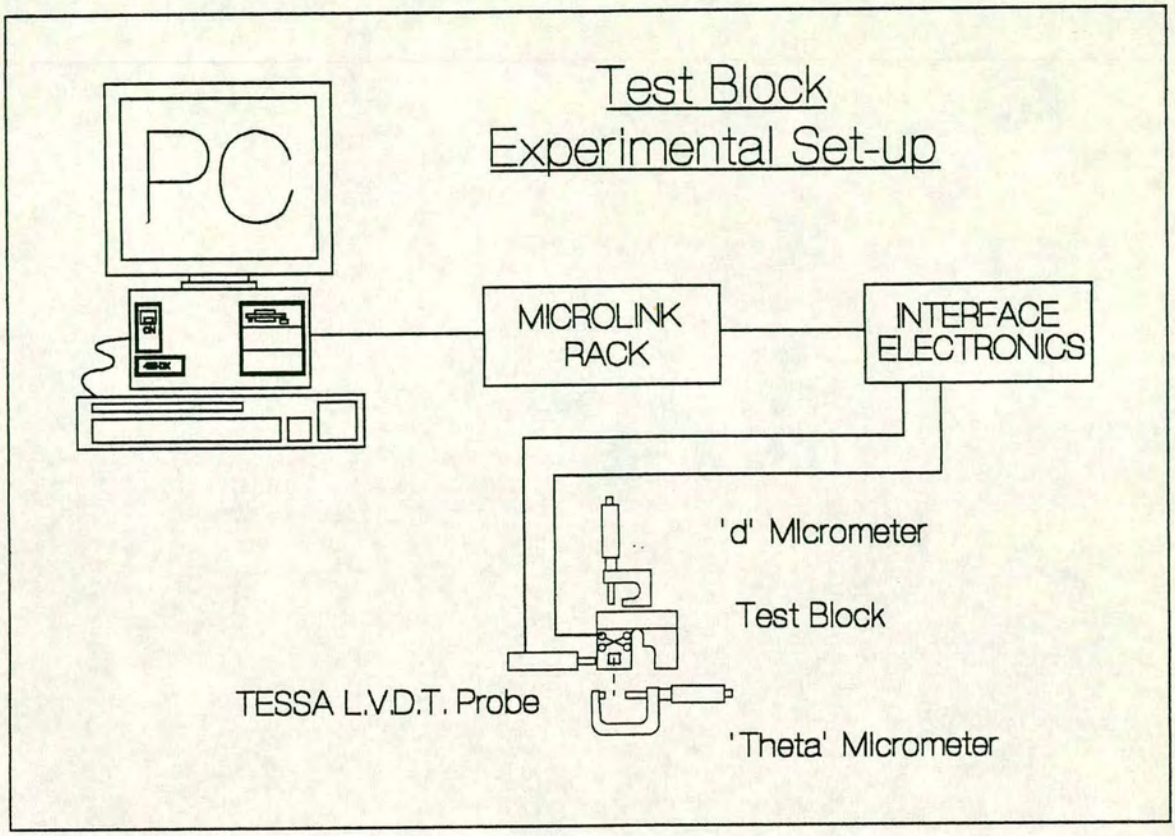

Figure 4.3 Testblock Experimental Set-up

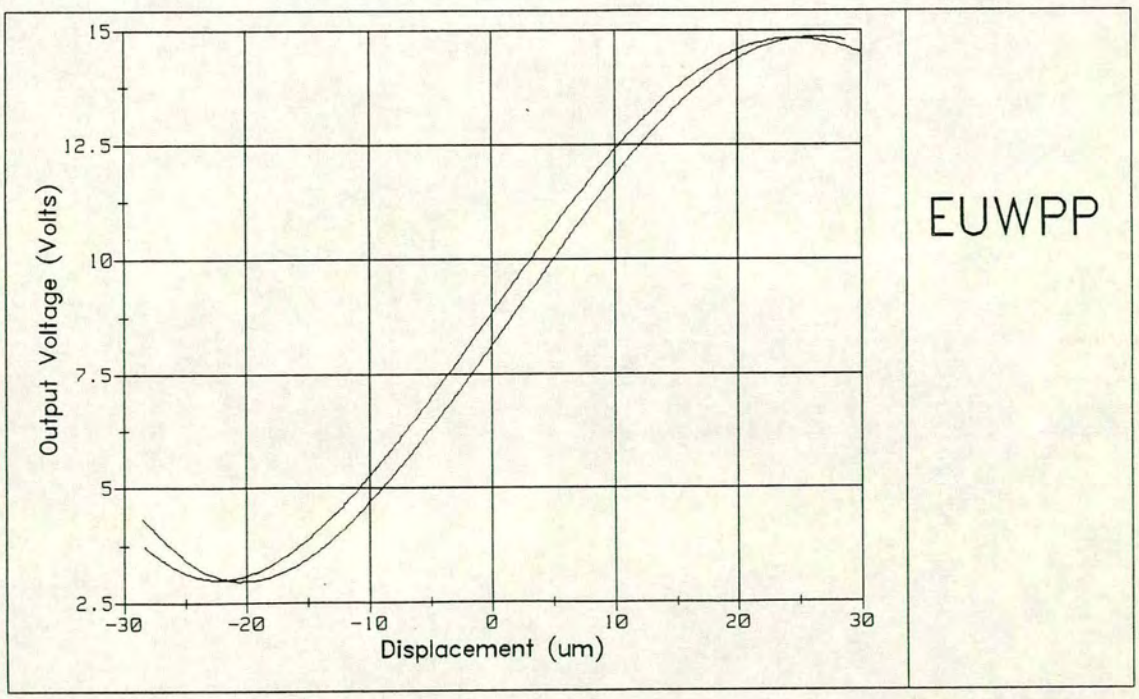

Figure 4.4 Repeatability Problems

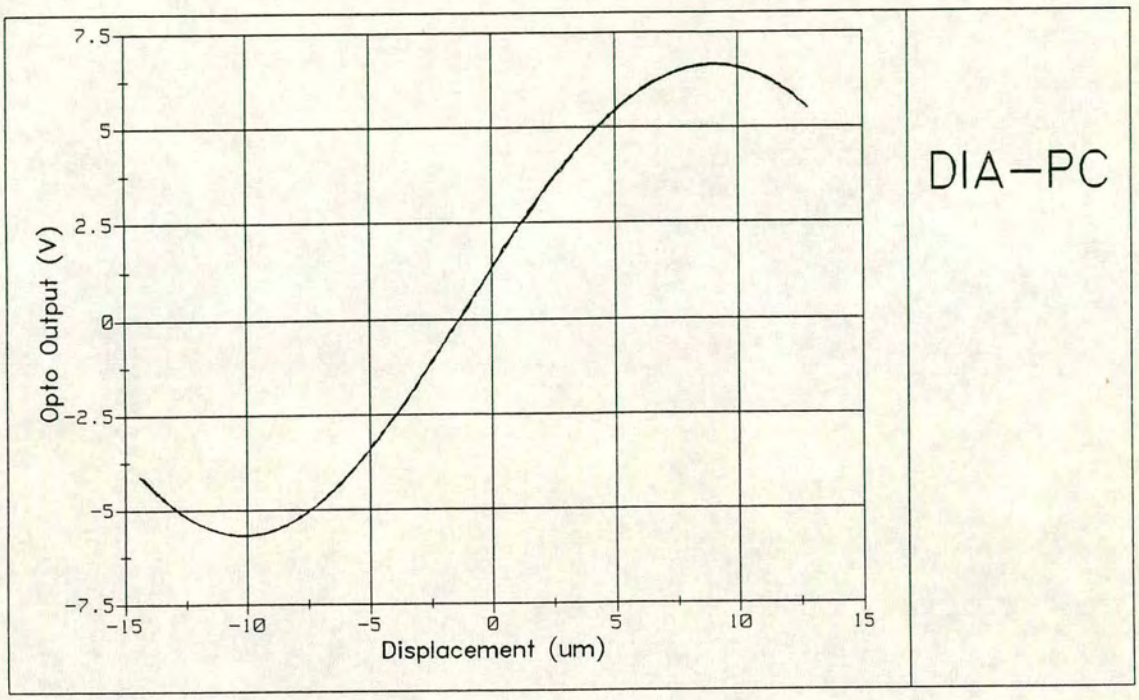

Figure 4.5 Final Repeatability

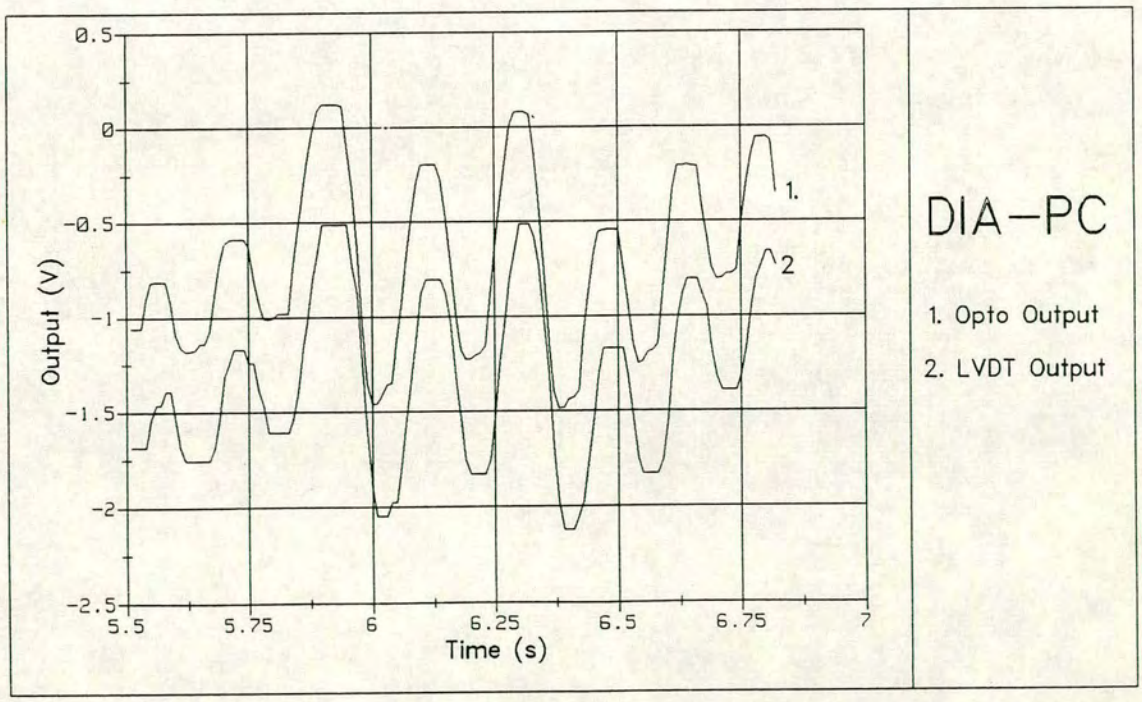

Figure 4.6 LVDT Phase Lag

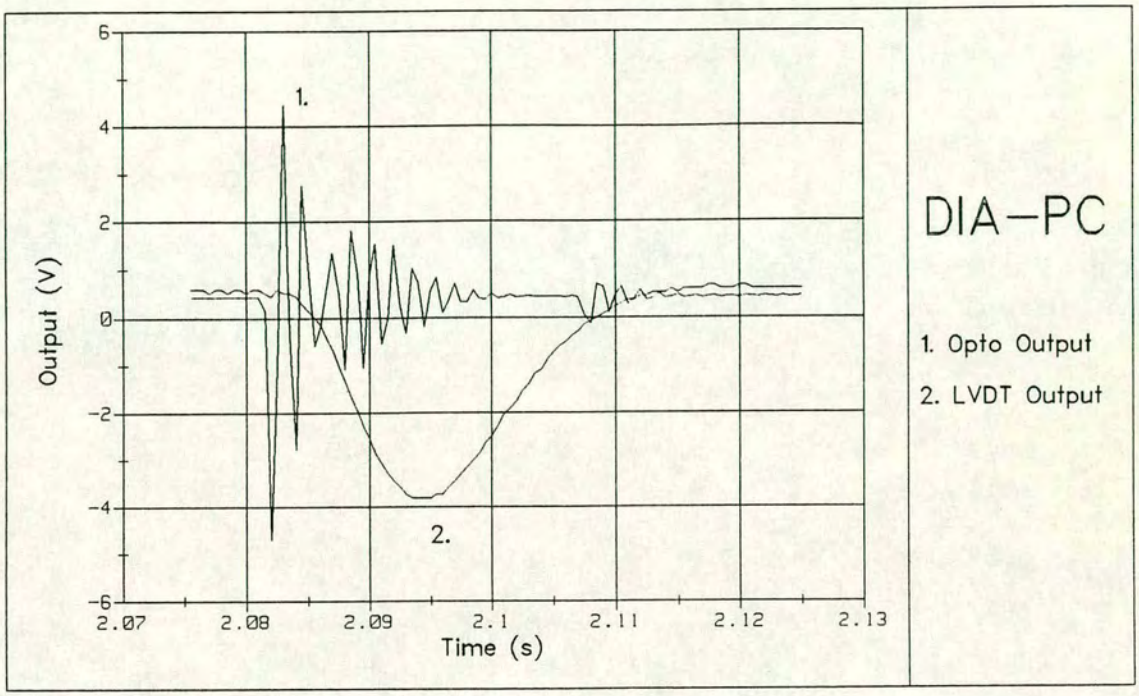

Figure 4.7 600Hz Free Resonance

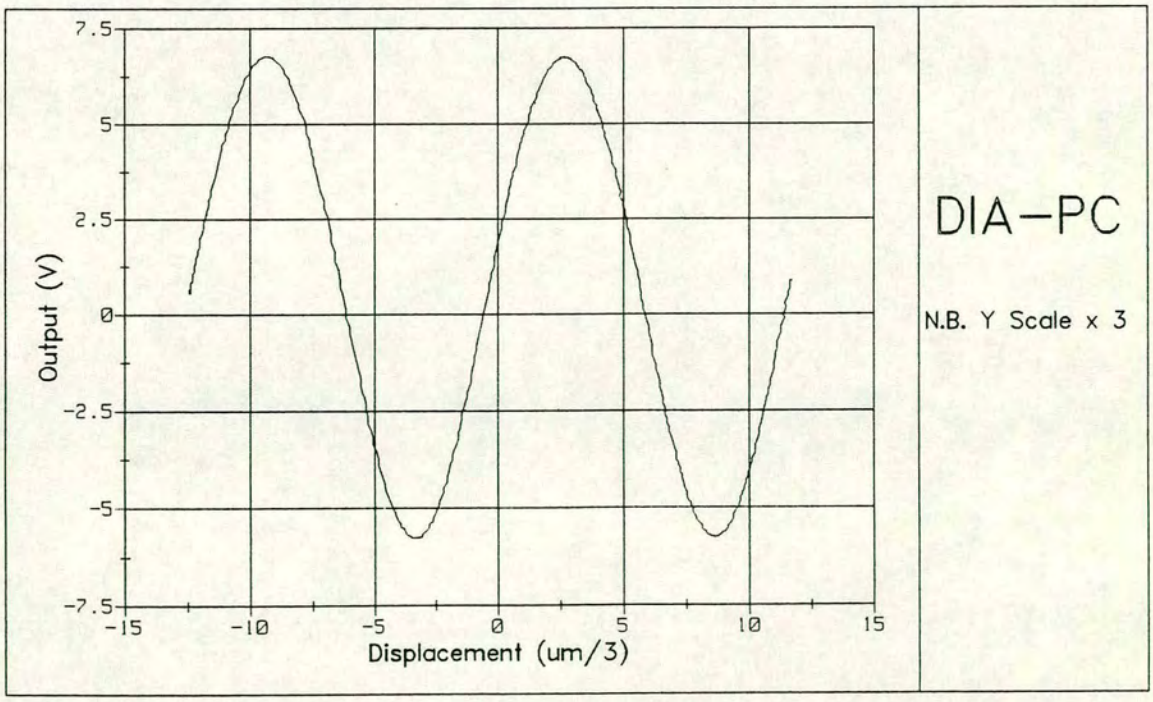

Figure 4.8 Opto Output over Two Complete Cycles

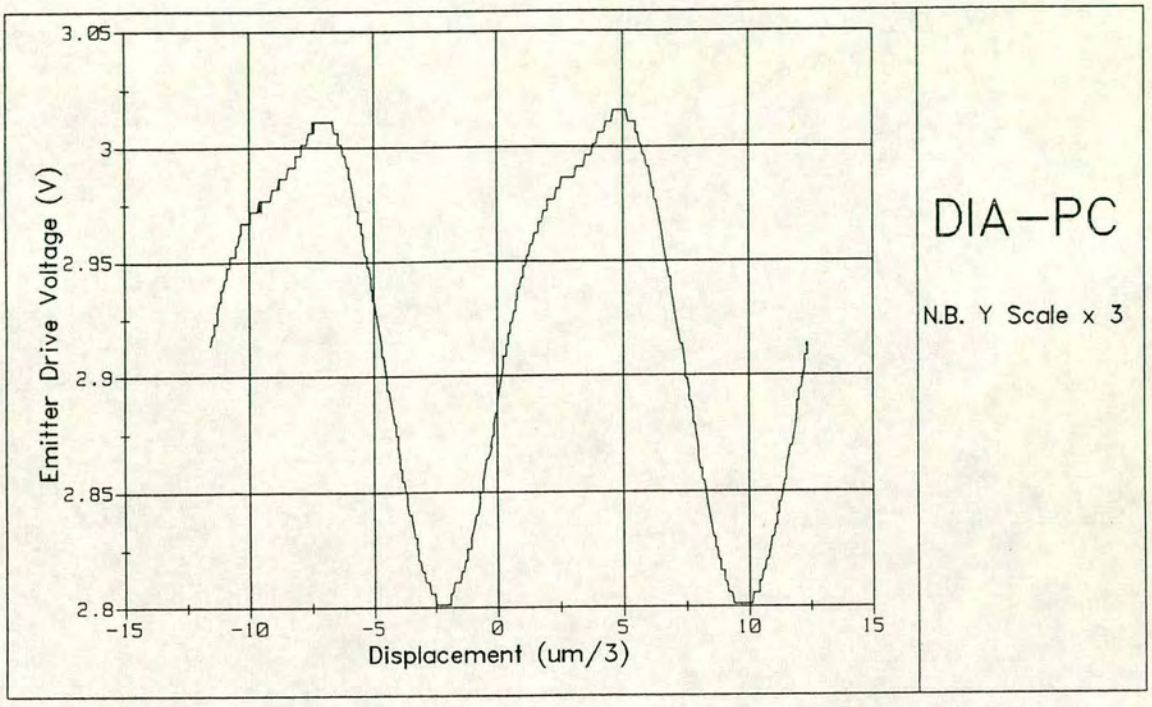

Figure 4.9 Emitter Drive Corresponding to Fig 4.8

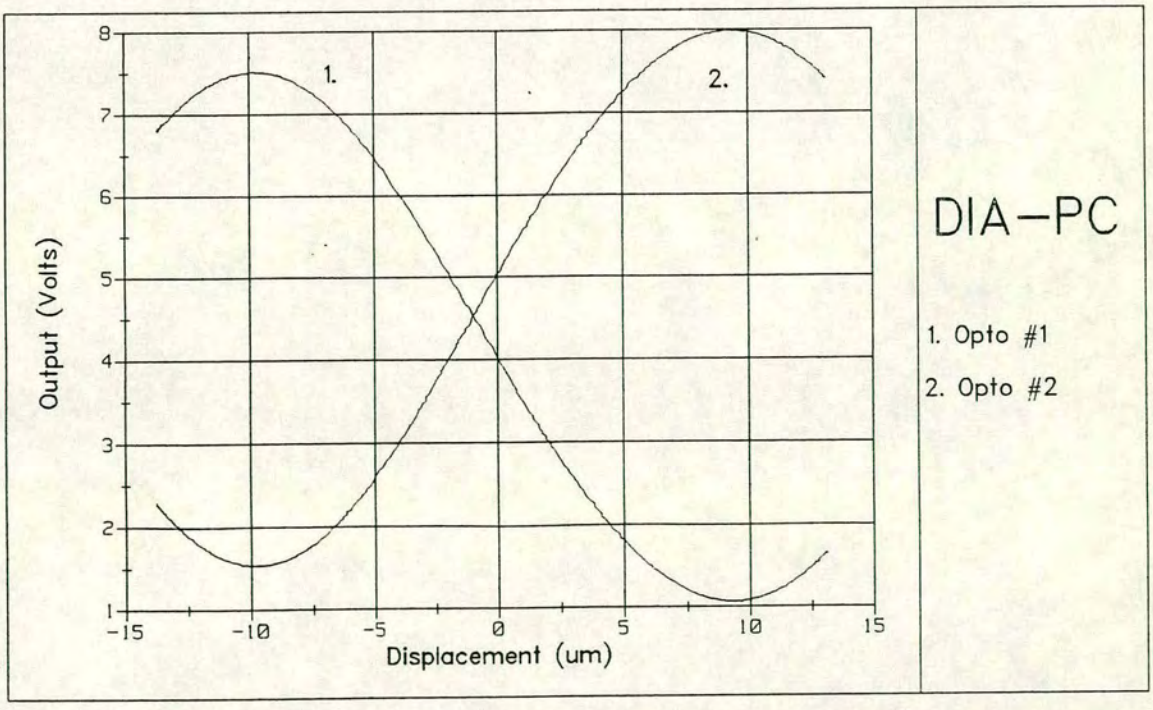

Figure 4.10 Individual Opto Outputs for a Similar Test

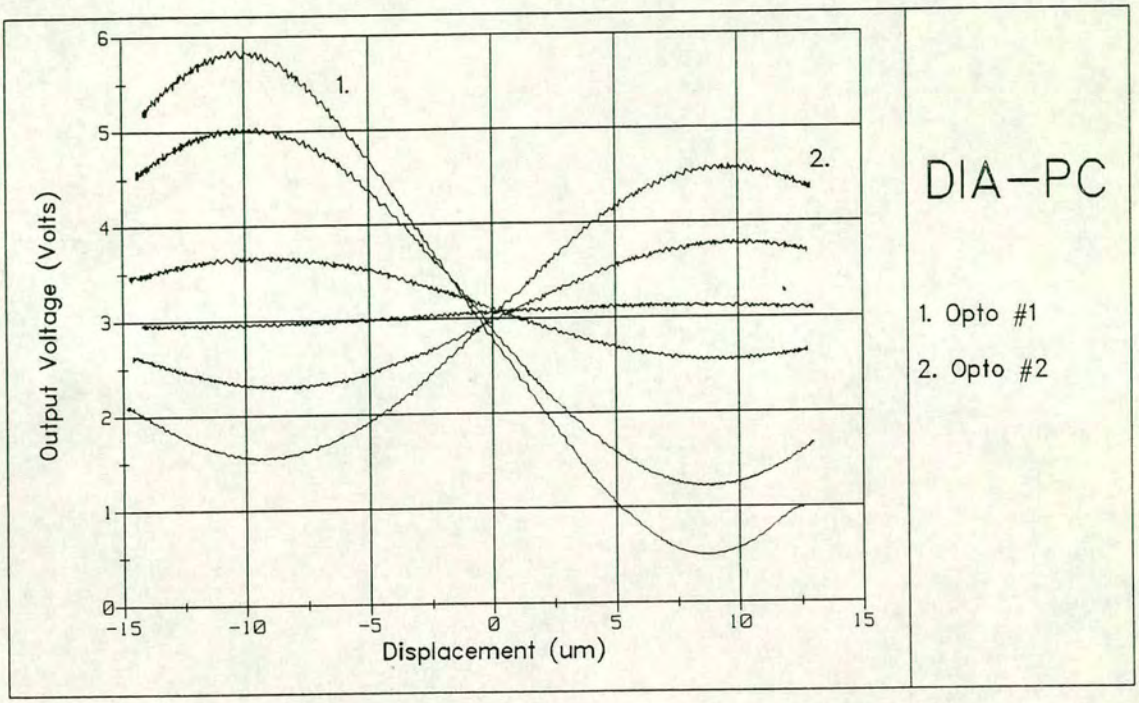

Figure 4.11 Open-Loop Opto Outputs

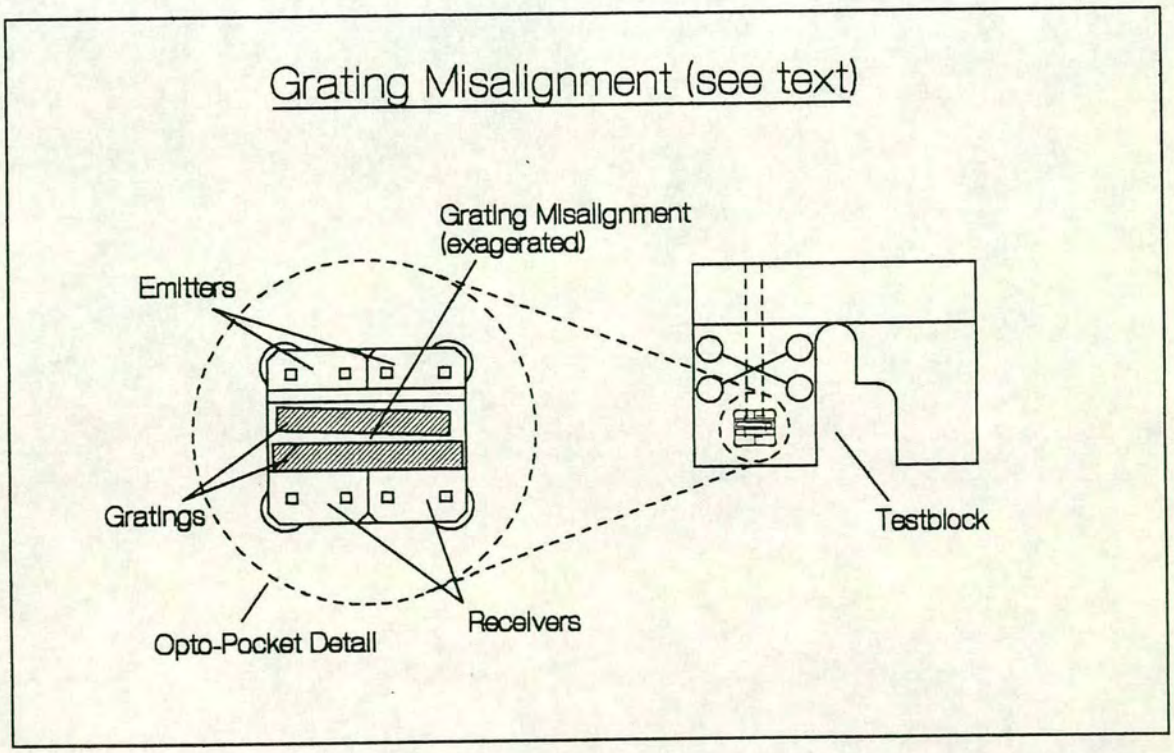

Figure 4.12 Schematic Grating Misalignment

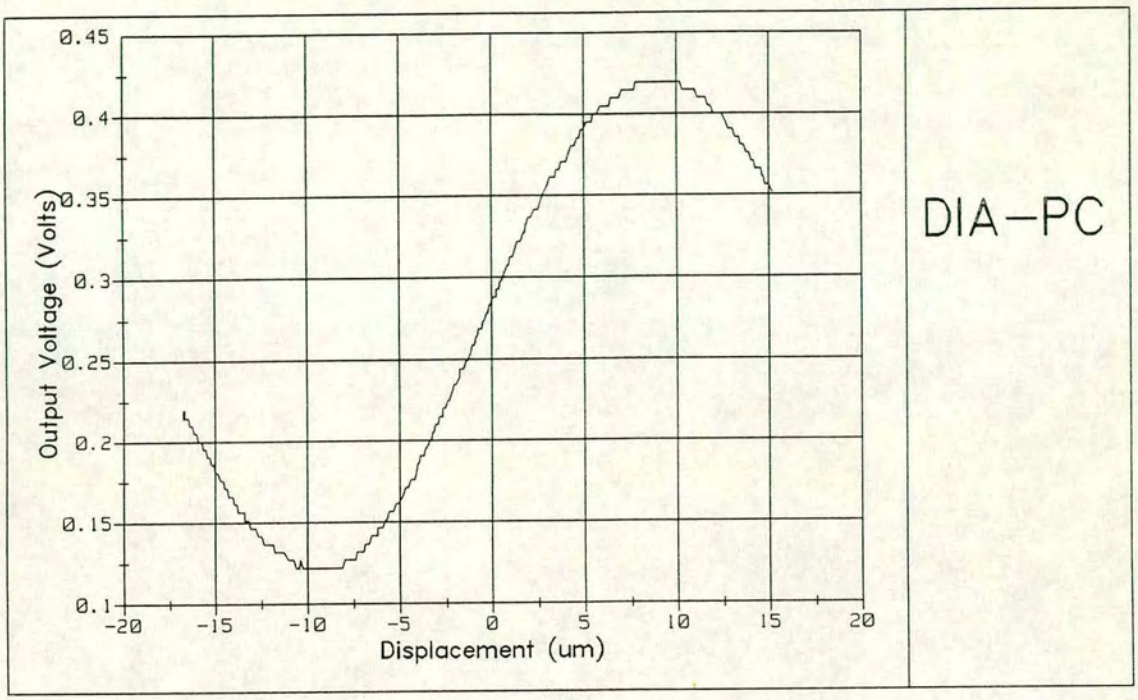

Figure 4.13 Improved System Symmetry at Large 'd'

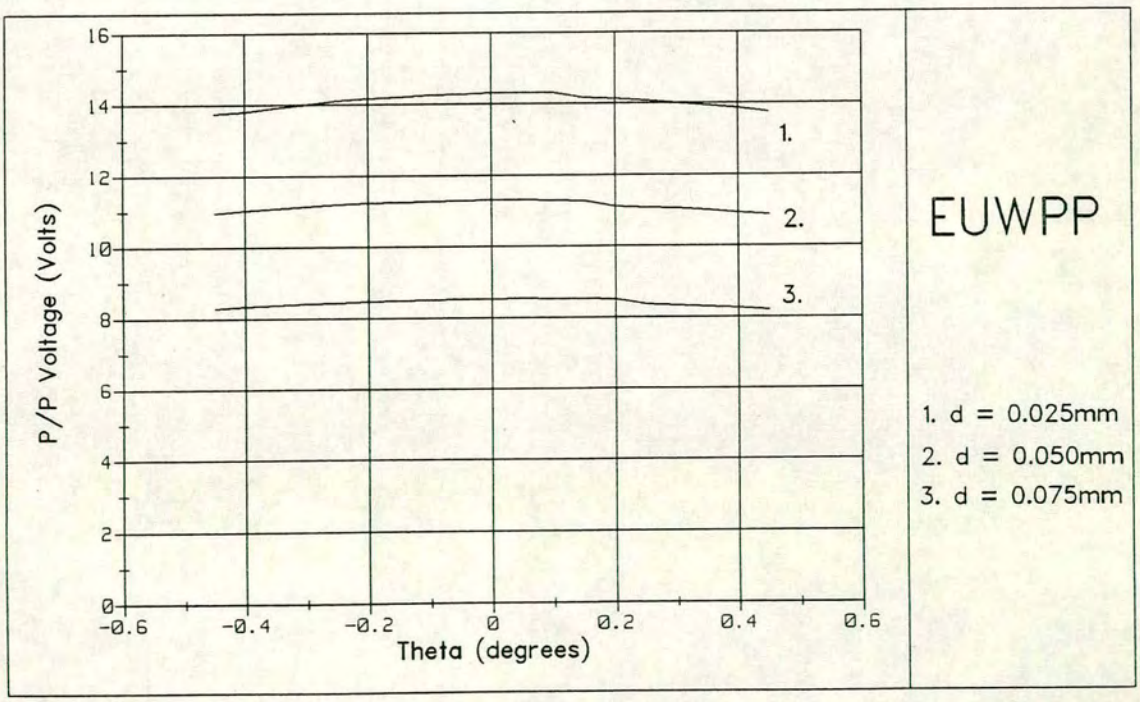

Figure 4.14 Peak/Peak Range for 10 lines/mm

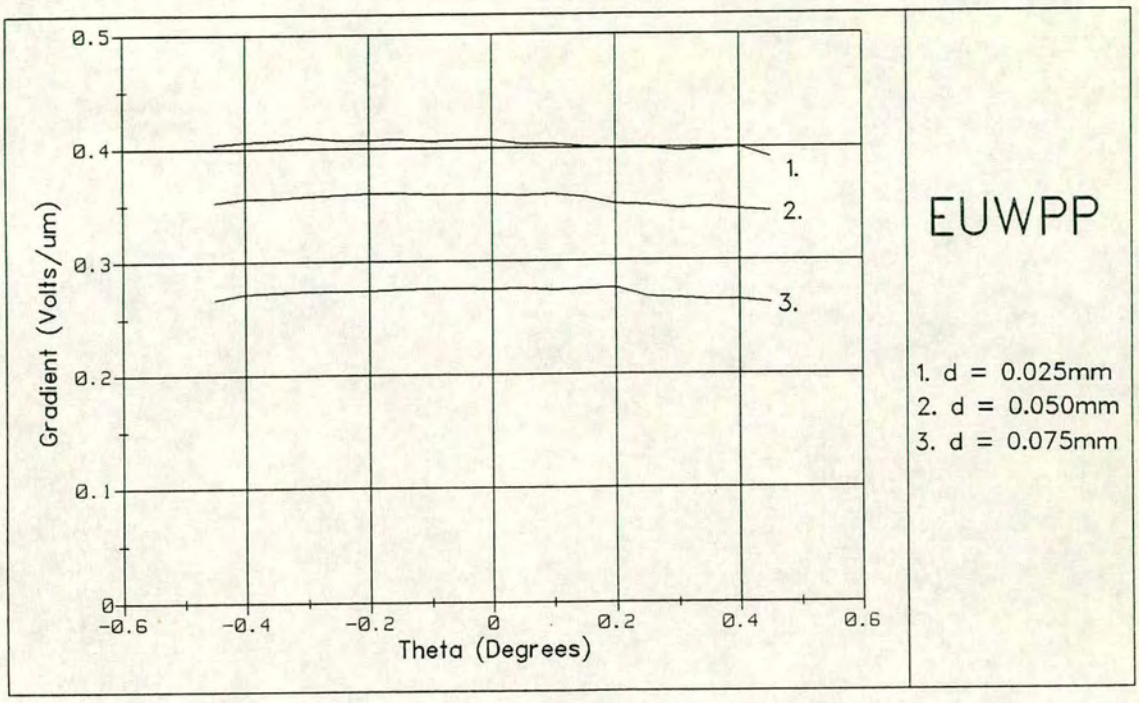

Figure 4.15 Peak Sensitivities for 10 lines/mm

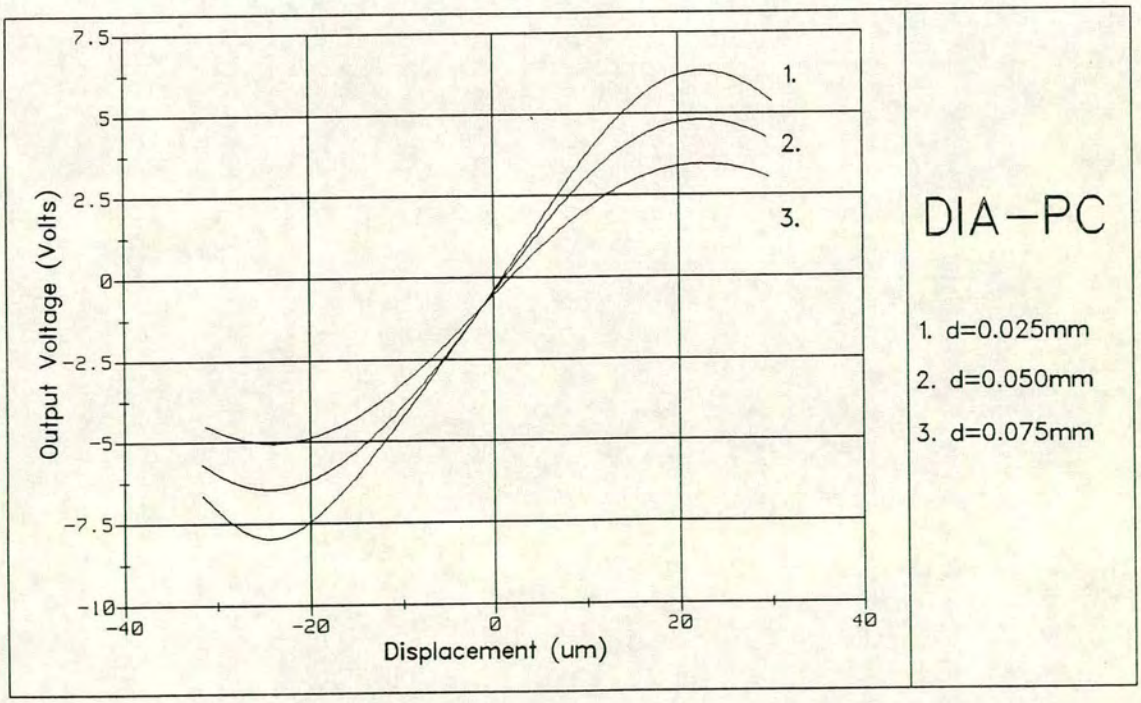

Figure 4.16 Individual Maximum Curves for 10 line/mm

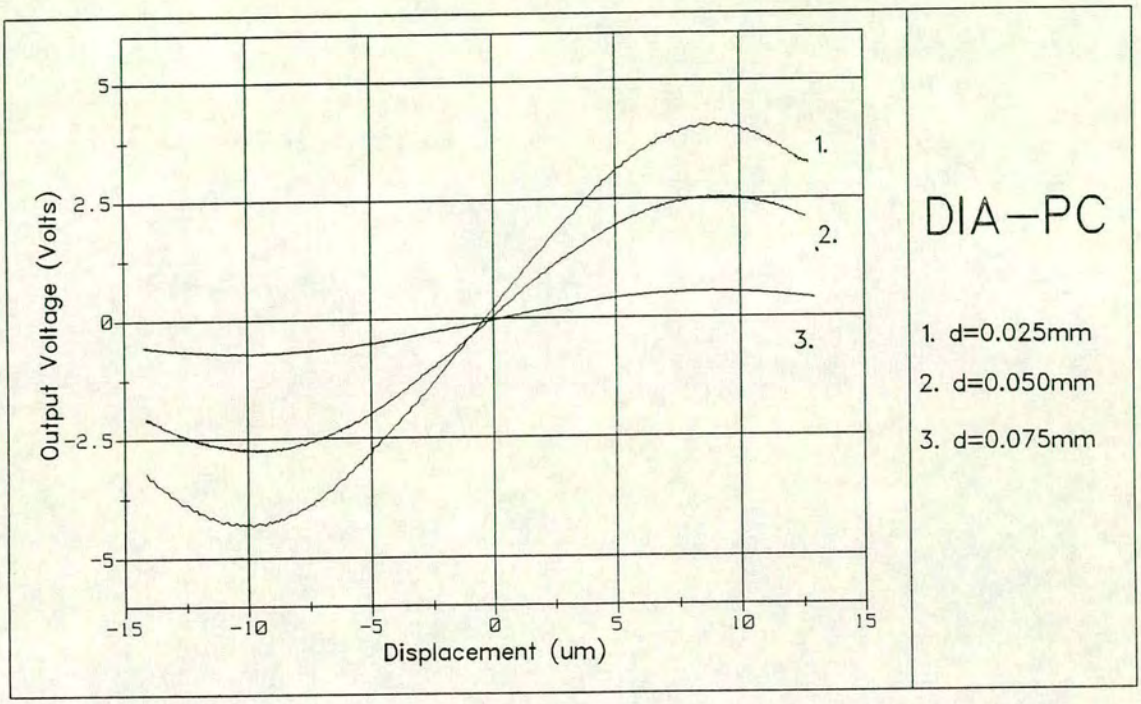

Figure 4.17 Initial Tests with 25 lines/mm

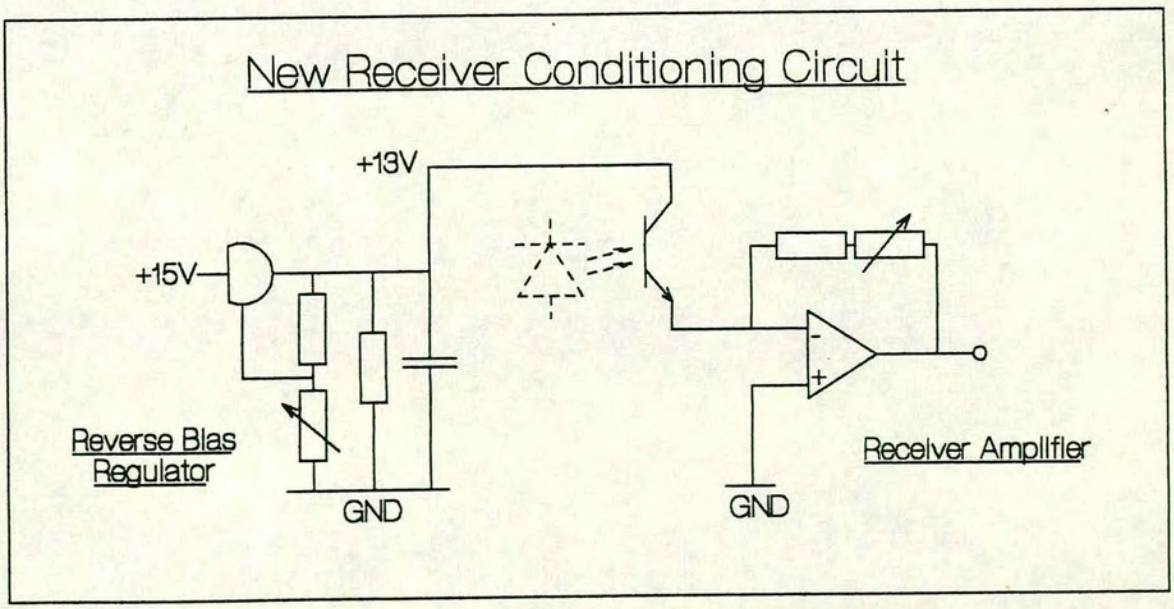

Figure 4.18 New Receiver Conditioning Circuit

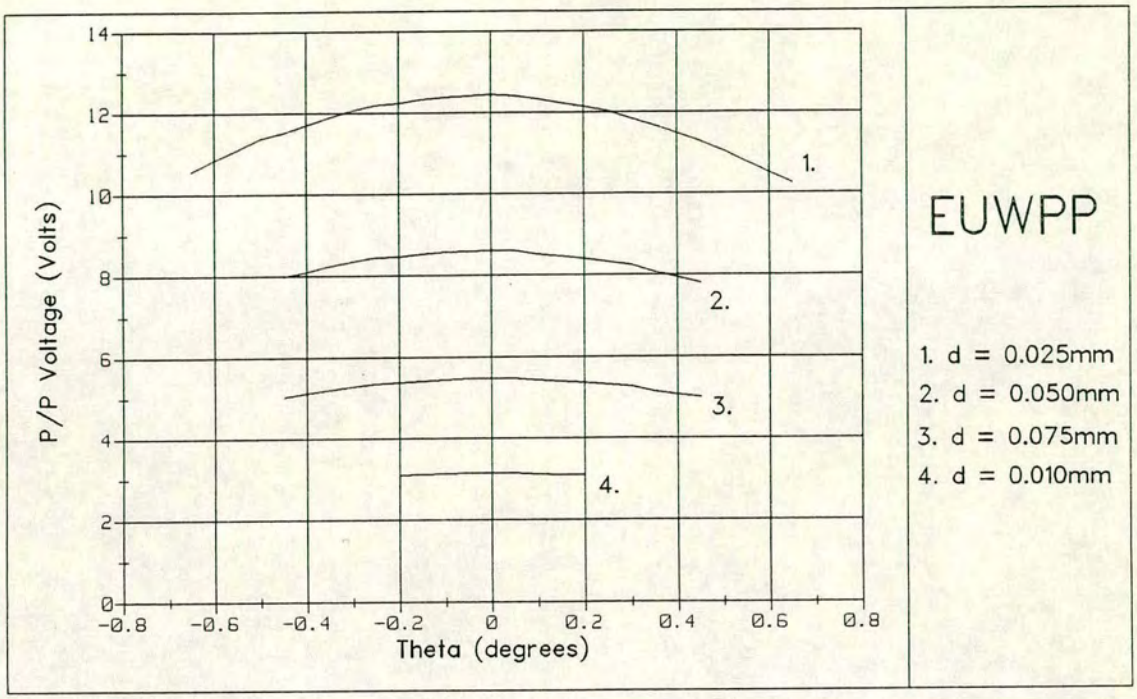

Figure 4.19 Peak/Peak Range for New Optos and 25 lines/mm

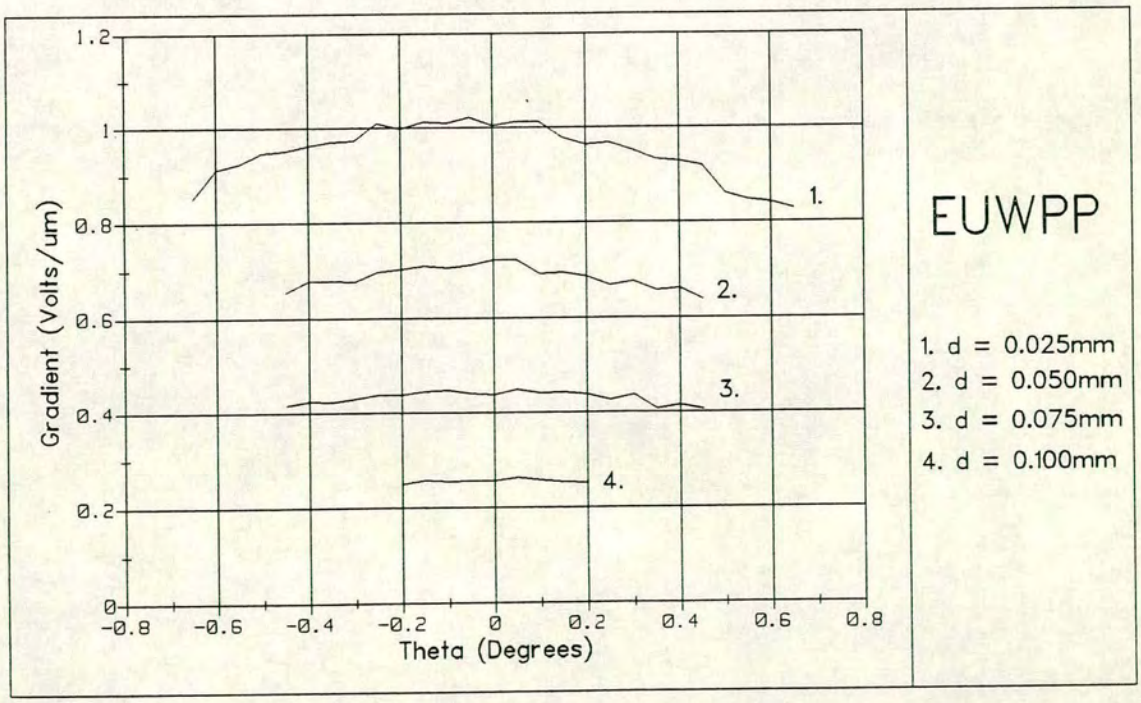

Figure 4.20 Sensitivity for New Optos and 25 lines/mm

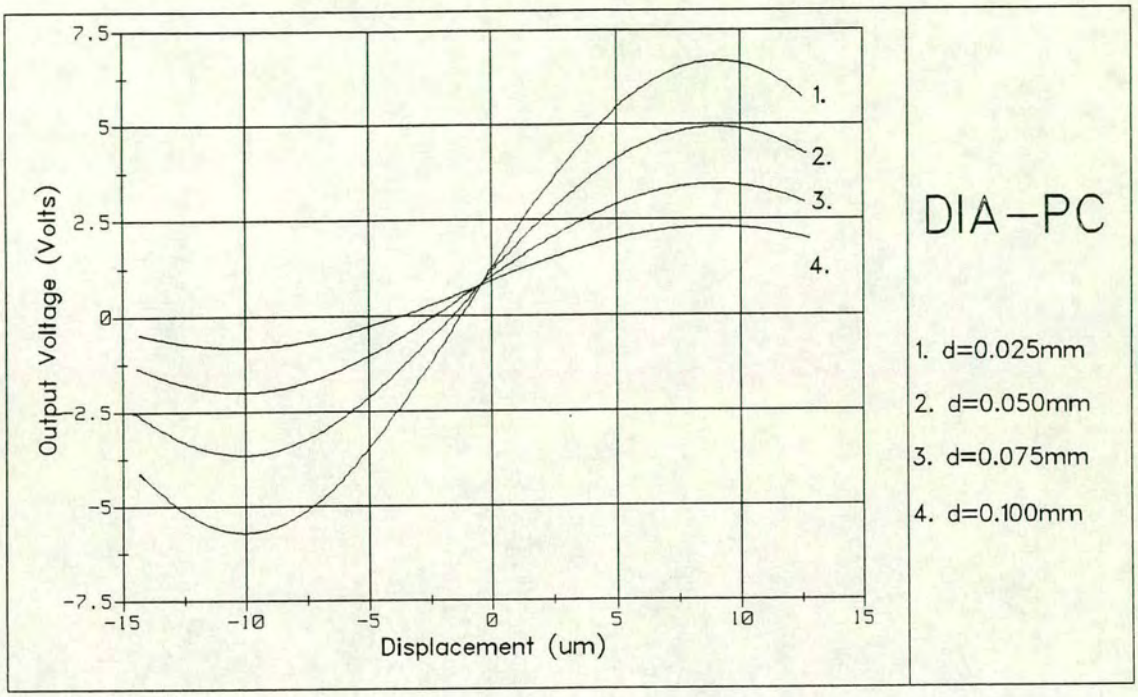

Figure 4.21 Individual Maximum Curves for New 25 lines/mm

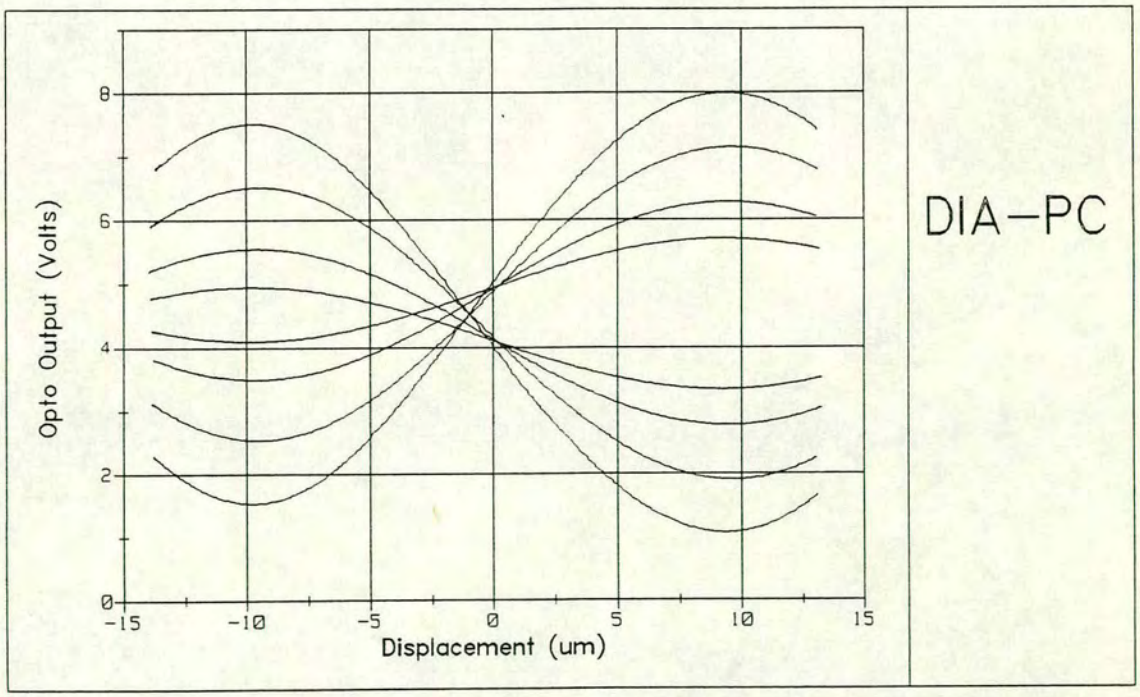

Figure 4.22 Individual Opto Outputs for Same Case

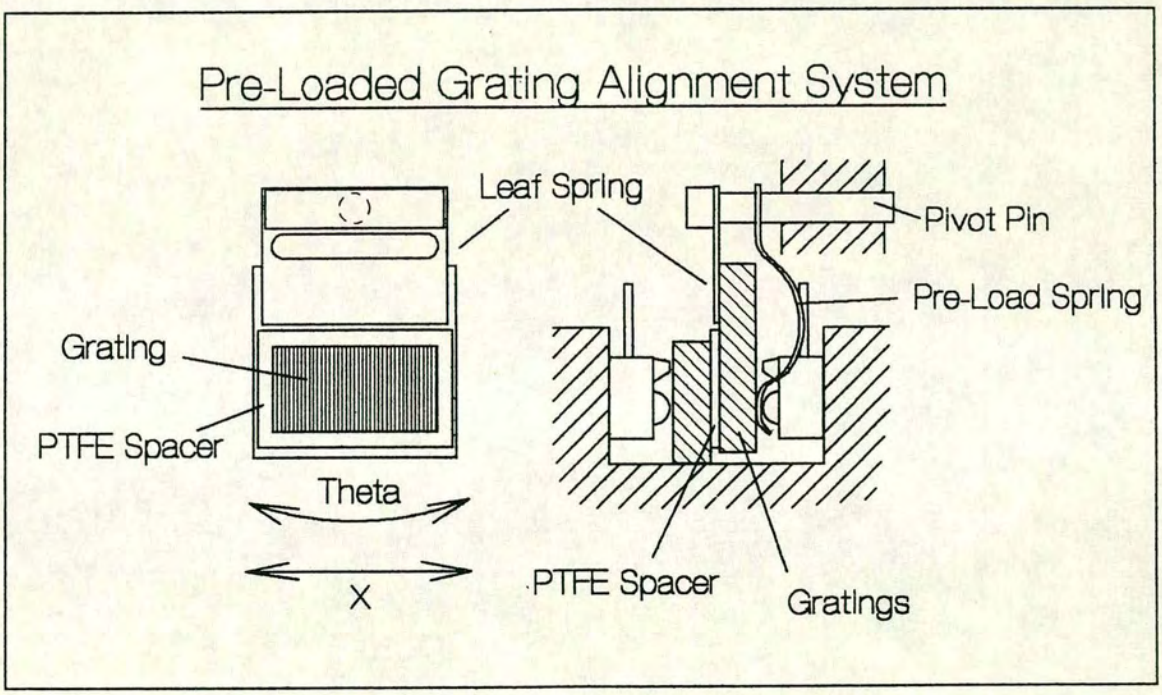

Figure 4.23 Pre-loaded Grating Alignment System

Chapter 5. Prototype Development

5.0 Chapter Summary

This chapter presents a record of the prototype development programme.

Design details, assembly procedure, performance figures and resulting development considerations are discussed for each of the individual loadcells.

The chapter concludes with a critical review of the development process including a discussion of positive and negative aspects of the approach used.

5.1 Notes on Performance Testing

Accurate quantitative assessment of the performance of the series of prototypes was impossible due to the lack of suitable facilities. Initial appraisal was on the basis of performance in a representative operating environment. This was usually in a heated room, subject to draughts and other general temperature transients. However, this rough and ready technique provided enough qualitative information to determine whether the cell under test was performing satisfactorily.

With the dramatic performance improvements achieved with later models a more rigorous method of testing was sought. The best that was available was the Wavepower Project "clean" room with its crude temperature control system. This allowed temperature to be loosely controlled within the range 21 C - 28 C. However, the test loadcell was still subject to local draughts. The results from tests in this environment gave a better idea of the thermal characteristics. However, proper transducer test facilities would be required for a full appraisal of all performance parameters.

5.2 Loadcell #1, Initial Prototype

With the conclusions and recommendations of the testblock series taken into consideration the first prototype design was drawn up. Several features were included in the design to allow disassembly after initial testing.

5.2.1 Design Details

The initial prototype is shown in cross section in Figure 5.1. A view of the various components is shown in Figure 5.2.

The basic arrangement is as described in the preceding sections. The opto components are housed in the central column linking the pair of diaphragms.

The outer casing is milled square after turning to reduce size while still maintaining a reasonable bearing length for the pivot pin, and to allow simpler cable exit via the then preferred method of case mounted connector socket.

The front diaphragm is machined as part of the outer casing to reduce hysteresis, part count, assembly time and size. This could lead to potential problems with residual stress in the casing causing popping of the diaphragms. Consultation with the British Stainless Steel Advisory Centre indicated that this was unlikely to be a problem.

However, to guard against any discontinuities it seemed prudent to pre-bias the two diaphragms against each other to ensure that popping can never occur within the measurement range. In this case the pre-biasing is achieved by machining the central column slightly shorter than the primary bore in the outer casing.

The required biasing is only a couple of times the full-scale deflection. However, realistic machining tolerances dictate a prebias of around 1/50mm. This has the adverse effect of reducing the overload capacity to around twenty. Closer tolerances are achievable if the components are ground to length, with a corresponding increase in price.

The rear diaphragm locates in the secondary bore against the machined face. In the prototype it is clamped in place by the rear boss to allow disassembly. In a production version the diaphragm would be bonded in under load.

The central column contains all the opto components and the receiver grating. Machining the opto pocket is a problem due to its aspect ratio. The pocket needs to be machined with the smallest cutter practical to allow access to the corners without undue weakening of the column.

The testblock pocket was machined using a 3/32" long series slot drill giving a maximum cut depth of approximately 8mm. The machined depth required for the real unit is 10mm. Changing to a larger cutter would be feasible. A better solution, giving lower overall material removal, was pre-machining a clearance slot across the column to give peripheral clearance for the cutter to machine to its maximum reach of 12mm.

Axial alignment is ensured by the locating bosses at each end.

The second grating is mounted on a pin pivoted in a reamed hole. In the prototype this is clamped by a set screw via a teflon pressure pad to prevent damage to the pin.

Mounting of the unit is via an M4 stud at each end. In a production version these would be machined as part of the respective pieces.

5.2.2 Assembly

The assembly procedure is simple in concept but in practice it proved difficult.

The opto flying leads are fine multi-stranded wire to reduce parasitic forces and prevent fatigue failures.

The emitters and receivers were bonded to the aperture plates and then their rear faces milled coplanar to the front.

The optos were then mounted in the pocket with the receiver grating. They were held in place using a PTFE spacer to ensure alignment was maintained as the glue set.

The column is then clamped to the rear diaphragm before insertion into the case.

The second grating was jig glued to its mount block perpendicular to the pivot pin. These were then inserted into the gap and the central column rotationally aligned before clamping. This proved to be difficult. Alignment was hard to maintain as the end screws were tightened. However this was eventually satisfactorily achieved.

This whole procedure was hampered by the limited visual and physical access to the pocket.

As explained earlier, this operation was initially performed dry to allow subsequent disassembly.

5.2.3 Performance

Initial trials showed a jumping of the output after high load conditions, this was attributed to relative movement

of the diaphragms and central column. The unit was re-assembled with industrial 2-part epoxy on all joints.

In this form initial indications were very favourable. There was a fair amount of drift as the epoxy glue joints cured but this was expected. However, after a cure period of 48 hours the drift still remained. The output variation seemed to be temperature related and in the standard room conditions described earlier large fluctuations of as much as 10-15% full scale output (FSO) were noted. On application of a point heating load, such as a pre-warmed block or simple handling, rapid output transients of over 10% FSO were observed. Some transient drift was expected with point heat loads, however the magnitude observed was disappointing.

Other negative performance aspects were identified. The loadcell exhibited large hysteresis and creep characteristics, around 3-5% FSO This was probably due to creep within the highly stressed glue joint at the inner rim of each diaphragm.

Overall the performance of Loadcell #1 was very poor.

5.2.4 Development Considerations

The problems encountered with the manufacture, assembly and operation of the initial prototype led to a series of improvements to the design of the second unit.

Loadcell #1 proved to be very difficult to manufacture. It seemed desirable to reduce the part count and the intricacy of the individual components. Assembly proved to be much more difficult than expected as explained earlier. This was mainly due to the poor access to the opto-pocket within the casing. The poor performance was attributed to the clumsy layout and the clamping of the inner rim of the rear

grating leading to the observed creep, hysteresis and drift. The square casing requires a lot of material removal and leads to a bulky, heavy unit.

5.3 Loadcell #2

These various problems were addressed in the second design.

As discussed a major perceived shortfall in the previous design was the lack of access to the opto components and gratings. A much more open layout was sought, with most of the fiddly assembly operations done before the two halves of the opto set-up were brought together and aligned.

Also desirable was reducing the number of bonded interfaces within the system. A one piece central column and diaphragm unit seemed the most promising solution. Welding or brazing of the main components seemed a more stable assembly method, however there were serious concerns over local distortion due to uneven heating and cooling during assembly. Also the mechanical properties of the diaphragms could be compromised.

The Physics workshop have a facility for vacuum brazing, a much more controlled version of standard hard brazing. The unit is assembled with a bead of bronze filler paste around each joint. Critical areas are masked off with a stopper paint to prevent contamination. The unit is then heated slowly in a vacuum giving a very even temperature rise and preventing oxidisation. Once at brazing temperature the system is allowed to "soak" for a period of time before cooling over several hours. A fuller description of the process can be found in [9].

With these factors in mind the design of Loadcell #2 was drawn up.

5.3.1 Design Details

The design is shown in detail in Figure 5.3, the important features are discussed below.

A cylindrical case was chosen. The opto-pocket was dropped in favour of separate mounting of the two halves of the optical system. The pair of emitters are mounted in a recess in the one piece central column/diaphragm block. The receivers together with one grating are mounted on a crescent shaped piece, separate from the deflecting mechanism. This block has the same outer diameter as the main casing. The second grating is now mounted on a pin in a reamed bore in the central column. This can be inserted, after jig gluing, through a port in the main casing. An extension pin is then used to set the grating clearance and angle. A thin outer casing to close the holes in the main casing after assembly completes the unit.

5.3.2 Assembly

The central column was first vacuum brazed into the main casing by the Physics workshop. The pre-biassing of the pair of diaphragms was omitted. If "popping' was observed, future models would be pre-loaded while brazing. In operation no such effect was observed. This change has the added advantage that overload capacity rises to between 40 and 50 times the rated load. The time/temperature profile required was of a form that would usually be associated with an annealing or normalising process. It was presumed that this would adversely affect the mechanical properties of the EN56 stainless steel. However, relevant literature [10] seemed to indicate that the sluggish phase changes typical of many stainless steels could mean that material properties may be improved under such conditions. To determine the effect of the process on the EN56 components a test piece were placed in the vacuum chamber during

brazing. A second similar piece was kept outside as a control. The pieces were subsequently tested in the Lloyd tensile tester in the Department of Mechanical Engineering, Edinburgh University. The results are shown in Figure 5.4.

The tensile test shows that there indeed seems to have been a large improvement in the yield and ultimate tensile stress after heating in the vacuum brazing furnace. More samples would need to be tested to show that this is a reliable result. If this improvement is consistent, further increases in the overload factor would be available.

The new design is assembled using the following procedure. The opto components and receiver grating are first bonded into their housings. The second grating on its pivot pin is then inserted with slow setting epoxy.

A jigging block was made to facilitate subsequent assembly. This is also shown in Figure 5.5. The crescent receiver block is offered up to the edge of the port in the main casing with a small amount of rapid setting epoxy. This assembly is then slid into the jig. The emitter grating pivot pin extension is inserted through the small pinch block and screwed in to the back of the main pin, aligning the casing, which is then clamped using the main pinch block. Gently pushing the pivot pin causes the crescent block to slide around the jig until the gratings are co-planar. The pin is then clamped in this position until the rapid set epoxy has cured. Grating separation and angle are then set as before. When the grating pin epoxy has set the complete cell is removed from the jig and the outer casing bonded on to complete the unit. The opto leads are lightly clamped and bonded in the slot in the outer casing, providing strain relief.

The whole process was very easy to perform and was a vast improvement on the original prototype. However, it was still time intensive.

5.3.3 Performance

The performance of Loadcell #2 was not much more promising. Drift, hysteresis and creep of the same order of magnitudes were noted. In addition the cell was even more sensitive to point heat application. Output swings of up to +-30% FSO were noted for the same local temperature transients as before. The persistence of these problems was presumed to be due to the large glue joint between the inner and outer casings.

In addition direct loading of the loadcell body induced large outputs, this was due to deflection of the thin casing directly affecting alignment of the gratings.

Once again performance fell far short of targets.

5.3.4 Development Considerations

Despite the persistence of drift and the sensitivity of the cell to external loads on the casing, Loadcell #2 was seen as a very positive step in the right direction. The main problems to be addressed by the third prototype were as follows. Although straightforward the emitters still had to be glued into the central column through the small casing port. The emitter leads could be prone to fatigue in applications where vibrations are present. As discussed the thin outer casing seemed undesirable due to the problems with local heating and loading. There was still a lot of glue involved in the overall assembly procedure.

5.4 Loadcells #3 & #4

Loadcell #3 was designed with these factors in mind. The concepts tested in Loadcell #2 were developed but with a major change in configuration. The main problems with the second prototype seemed to be due to the ports in the casing between the diaphragms and the thin outer shell. These could be avoided if the optical system was placed behind, instead of between, the two diaphragms. This was deemed to be acceptable because neither of the preceding prototypes seemed to have problems isolating off-axis loads and bending moments. This change in layout allows a much simpler scheme to be used. The resulting design is shown in Figure 5.6.

5.4.1 Design Details

The diaphragm/column unit is now a much simpler piece. The casing is easier to machine being open at both ends, has thicker walls and is un-breached between the two diaphragms. The only penetration is the small pivot pin access hole which doubles as the cable exit after assembly. All the optical components are mounted in a crescent shaped block with the same diameter as the inner surface of the rear portion of the casing. The deflecting grating is bonded into the "fork" in the rear of the central column. The rear cover completes the part list.

Loadcell #4 was identical to Loadcell #3 except the full-scale deflection was derated to 2.5um. Due to the continued drift problems discussed later, and continuing development of design ideas, it was never assembled.

5.4.2 Assembly

The deflecting column was vacuum brazed into the casing as before. A small vent from the front mounting hole was required to allow evacuation of the enclosed space.

The emitters, receivers and one grating can all be glued into the crescent block clear of the main body. The second grating was jig glued to the pivot pin as before. The assembly jig used for Loadcell #2 was modified for use with the new unit. The assembly procedure was similar before but turned out, as hoped, to be even more straightforward.

5.4.3 Performance

Loadcell #3 exhibited the worst overall temperature drift characteristics. This was probably due to the very thick glue joint between the moving grating and its mounting fork. Output swings of in excess of +-20% F.S.O. were observed with the loadcell sitting undisturbed in the same conditions as before.

On a more positive note the response to point loading and heating were much improved. A relatively small output response of approximately +-5% was noted for similar temperature transients, and local loading effects were barely measurable. In addition hysteresis and creep were significantly less, although still present.

5.4.4 Development Considerations

The design concepts used in Loadcell #3 were generally seen as a positive step with exception of the fork mounting for the second grating. What was needed was a further reduction in the number and thickness of glue joints within the system. A careful look at improved methods of mounting the

optical components and gratings was undertaken. The aim was to eliminate glue joints that could lead to temperature induced drift of grating alignment.

5.5 Loadcell #5

As a more general change of approach to the problems encountered with the twin diaphragm configuration an effort was made to re-examine alternative configurations. One layout, that threw up the significant ideas that led to the eventual design of the successful loadcell, was made but never assembled.

Loadcell #5 was based around a simple cantilever beam deflecting mechanism. This was viewed at the time as a serious compromise due to susceptibility to off axis loads and bending moments. However, the main ideas behind it seemed none the less sound and so it was made. The important features all centred around the method used to mount the optical components.

The key idea introduced was that of the eccentric opto can or cam. Emitters and receivers are mounted in eccentric cams. This retains the capability to bias the loadcell output by altering the 'theta' alignment but has three important advantages over previous methods. Firstly the grating is glued to the large, flat outer face of the can. The glue joint itself is of negligible thickness and the grating cannot move out of plane with the axis of the cam. The second advantage is that the symmetry of the glue joint between the cam and the bore should prevent any expansion related drift of grating position. Finally, the system allows the pre-assembly of complete emitter and receiver 'heads', reducing assembly time and problems to an absolute minimum.

The re-introduction of a positive locking mechanism for component location was also seen as a sensible precaution.

5.5.1 Design Details

The full design is shown in Figure 5.7.

A long clearance bore up the centre of the cantilever beam allows a single emitter to be mounted in an eccentric pin located in a bore in the fixed end of the system. The pair of receivers are mounted in an eccentric can, as discussed above, in an opposing bore in the free end of the cantilever. The gratings are mounted to the respective faces of these cams. The small eccentricity available is compensated by the fact that both sides are adjustable.

The use of a single emitter only became possible when a new style of receiver package was found. This reduced the collimation errors to an acceptable level.

HE15 aluminium alloy was chosen in preference to EN56 to make the unit due its superior thermal conductivity properties, and to reduce problems with milling the deep, narrow slot.

As mentioned above Loadcell #5 was never assembled. This was due in part to the reluctance to give up hope of sorting out the problems with the more elegant diaphragm layout. Also it was felt that the long emitter pin was relatively well insulated from external temperature transients and so may have led to problems. However, this design can be looked on as the conceptual breakthrough which eventually cracked the nut.

5.6 Loadcell #6

As mentioned above there was a reluctance to abandon the cylindrical package style. It was decided that another attempt should be made using this configuration in conjunction with the optical advances made with the design of Loadcell #5.

5.6.1 Design Details

Figure 5.8 shows the layout of Loadcell #6. The design is fundamentally the same as #3 & #4 with different optical mounting. The deflecting grating is now mounted on a substantial "tongue" milled as one piece with the central column and diaphragms. This sticks into the milled compartment at the rear of the cell. The extra depth left by milling rather than boring out the rear cavity is used to provide sufficient bearing length for the receiver cam. A single emitter is mounted directly in a simple opposing bore, and shines through the port in the grating "tongue". Once again a rear cover completes the design.

A de-rated full-scale displacement of 2.5um was chosen again to improve the chances of success.

5.6.2 Assembly

Unfortunately at the time of assembly of Loadcell #6 the vacuum brazer was out of commission. Reluctantly the central spool was bonded in using a special thermo-cure industrial epoxy resin with superior properties to conventional two-part systems. However, this was a shame because it introduced an extra unwanted variable into the performance equation.

The rest of the assembly was by far the simplest and most trouble free of all the prototypes to date due to the modular design. The only remaining fiddly operation was the alignment and bonding of the deflecting grating to the tongue. However, even this presented little problem. A thin penetrating cyanoacrylate adhesive applied after alignment simplified the task and kept the bond line thickness to an absolute minimum.

5.6.3 Performance

Loadcell #6 exhibited the best overall performance achieved up to the this point. Drift was reduced to approximately 5% F.S.O. for similar conditions to previous tests. Hysteresis and creep were only slightly more marked, this was attributed to the fact that the diaphragms were glued in rather than brazed. Response to local thermal transients was still poor.

With the dramatic reduction in overall drift, Loadcell #6 was seen as a qualified success. However, the thermal performance was still unacceptably poor.

5.6.4 Development Considerations

Thus the performance was once again disappointing. Despite the many different approaches the double diaphragm configuration seemed particularly prone to temperature drift problems. This is probably due to the large dissimilarity in the grating/ambient thermal paths of the two halves of the optical system leading to very different relative expansion rates. In Loadcell #6 this would be compounded by the large thermal inertia of the grating tongue and the thermal barrier posed by the epoxy diaphragm bonds. Another possible source of problems could be the omission of a positive clamping of the receiver can. With

hindsight it would have been sensible to include a clamp screw. This would have provided more positive location and would have improved the thermal path between the can and the case.

Throughout the development phase there had been a positive effort to reduce the quantity and complexity of the machining involved. However, the single piece central column in any of its guises would be relatively time consuming and expensive to make accurately in quantity.

As discussed earlier the unit was much easier to assemble than its predecessors, however it was still felt that there could be improvements in the area. For example the double can arrangement discussed for Loadcell #5.

What was needed was a completely different approach to the problem with the overriding objective being to increase the symmetry of the optical system. This was to prove to be the key to the puzzle.

5.7 Loadcells #7 & #8

The configuration chosen was that shown in Figure 5.9. The important design features are discussed below.

5.7.1 Design Details

Loadcell #7 was a return to the simple, reliable deflecting mechanism used in the original testblock (Figure 4.1). The system was made totally symmetrical by replacing the pivot pin with a second identical mechanism placed above the first. Only one is loaded in normal operation, the other is included as a thermally symmetric dummy. This layout allows the entire loadcell body to be machined from a single block. The optical axis is now set perpendicular to the

deflecting mechanism to allow the components to be mounted in opposing cans similar to the receiver unit in Loadcell #6. The cans are clamped in place during bonding to ensure alignment is maintained. Aircraft specification aluminium alloy (HE-15) was chosen in preference to stainless for its strength, ease of machining and above all its superior thermal conductivity.

A dramatically reduced stiffness was chosen with a full-scale deflection of 10um. This allowed the use of the less critical 10 lines/mm gratings at a much larger separation. The increased deflection means that the overload capacity is significantly reduced, however, an estimated factor of safety of twenty was still deemed to be ample.

The single emitter style was retained but a more powerful and narrower angle infra-red emitting diode was found that greatly increases the current transfer ratio allowing the whole emitter system to run at a much lower drive current.

The new loadcell configuration has a number of important features and advantages.

The unit is now much simpler to make. All machining operations, apart from the freeing cuts, are simple planar milling or drilling/reaming operations. Alignment of the opto cans is ensured as the two holes are reamed as one before the block is weakened. Concerns over stress release destroying alignment when the block was "free-ed" proved to be unfounded, the reamer shank still passed smoothly through the bore after the cuts had been made. The slits were made by the Physics workshop, University of Edinburgh, using Electro-Discharge-Machining (EDM). This gives narrow accurate cuts and does not take significantly more time than conventional methods.

The parallelogram springs offer much better heat sinking and transfer than the diaphragms. This in conjunction with the one-piece aluminium alloy body allows temperature transients to be dissipated much more rapidly. The orientation of the gratings parallel to the springs means that the optical system is immune to relative length changes of the two halves. Theoretically the only steady state thermal error is the change in length of the short "bridge" between the two halves (formed by the main cut) leading to variation in grating separation. With typical variations of less than 0.5% of the grating clearance over a temperature range of 50 degrees C this effect should be insignificant. The emitter drive feedback loop also tends to reduce this effect.

Rapid asymmetrical surface temperature transients will lead to bowing in or out of the parallelogram arrangement leading to more serious grating separation fluctuations. The rapid sinking of such point heating loads reduces the severity of this problem.

In addition to favourable thermal characteristics the design has several other interesting and useful features.

The choice of which parallelogram to load gives instant mechanical polarity reversal. The high overload capacity in conjunction with loading both parallelograms allows small differential forces to be measured in the presence a large common-mode loads.

The thermal resistance of the springs is proportional to their thickness. Their stiffness, however, scales with thickness to the power of 2.5. This means that the two parallelograms can have very different stiffnesses without significantly affecting the thermal symmetry. This leads to

possibilities of making a dual range loadcell within a single package.

If mechanical clamping alone proved to be sufficient, one set of the expensive optical cans could be placed by the user in a number of different cheap bodies, again increasing the versatility of the system.

Overall the new concept was seen as an exciting new development with many possibilities for different general and specialist applications.

5.7.2 Assembly

Assembly is greatly simplified because now all the various optical components are put together outside the loadcell body. This also increases the accuracy with which this process could be carried out.

The two cans are assembled in much the same way as the receiver unit in Loadcell #6. The emitter was set back from its grating to improve the apparent collimation.

The new assembly sequence is as follows. First the receiver can is inserted into the case. The thick line in the middle of the grating is used to visually align the can which is then clamped lightly in place. The emitter is then inserted and the grating separation set using a micrometer as before. A light clamp is then applied to steady the can as it is aligned and biased to the centre of the range. Both screws are then tightened in stages. The output is monitored to ensure that an accurate zero is maintained. At this point a small quantity of penetrating adhesive could be introduced to the outer of each can to permanently fix alignment. This was not done on the prototype to allow dis-assembly for modification and diagnostic purposes.

After initial assembly experiments it was found that setting the grating clearance with the micrometer was unnecessary. Adequate alignment could be attained by gently moving the can in and out while rotating slowly about the zero point until the required output swing was achieved. This allows very rapid unskilled assembly with no jigging required.

Overall Loadcells #7 was by far the easiest to assemble and align.

5.7.3 Performance

Initial performance characteristics were very encouraging, after an initial settling period the loadcell output seemed to stabilise. Overall drift seemed to be around 2% FSO. Linearity appeared to be excellent and hysteresis was barely measurable. However, it was found that an error had been made in the spring calculations leading to a stiffness a factor of 5 less than the target. The calculations were checked and a new loadcell body made. Loadcell #8 was assembled and similar performance characteristics noted.

It was decided at this stage to transfer the unit to the more controlled conditions afforded by the Wavepower "clean" room to try and get a more accurate assessment of the temperature drift characteristics.

With the unit set up there and the temperature stabilised at 25C significant drift was still evident. A very slow, wandering response to local transients was noted. It was decided that these two characteristics may have been due to the dissimilar coefficients of expansion of the loadcell body, steel clamp screw and nylon pressure pad. To cure this an alloy screw and pressure pad were made and installed. This improved the performance markedly. Loadcell output seemed to be drifting less than 0.5% FSO with the

temperature held at 25 C. Response to local temperature transients showed a smaller output swing and a much faster subsequent recovery.

A crude test was carried out to try and estimate the temperature coefficient of zero drift. The room temperature was allowed to fall to 23 C before being ramped up to 28 C. This 5 C swing seemed to indicate that the drift was around 0.2% FSO/C. This was very encouraging but another effect became evident. If the loadcell was vigorously deflected the output showed a tendency to jump to a new zero value and then slowly drift back to the original null. This was attributed to movement of the opto cans due to the imperfect location afforded by the clamp screw system. Although a small drop of glue may have cured this it was decided that alternative clamping systems should be investigated.

5.7.4 Development Considerations

All aspects of the performance of the new configuration looked very promising. Holding the optical cans by mechanical means only was seen as a major advantage. This would allow the versatile scheme of using one set of opto cans in many different bodies. With this in mind a further prototype was made incorporating a more stable pinch block style clamping arrangement.

5.8 Loadcell #9

Loadcell #9 is shown in Figure 5.10.

5.8.1 Design Details

The design is identical to its predecessors in all respects with the exception of the can clamping arrangements as shown. A simple mechanical clamp is formed by pre-straining the pinch block so that it automatically grips the cans with no extra fastenings. The screw is provided to allow insertion of the cans and subsequent alignment. A full scale deflection of 10um was again used.

5.8.2 Assembly

Assembly procedure was the same as for Loadcells #7 and #8.

5.8.3 Performance

Initial Tests

Initial tests showed that the loadcell appeared to be exceptionally stable. Several 5 C step tests seemed to indicate that the temperature coefficient of zero drift could be as low as 0.1% FSO/C. There was no sign of steps in zero point even after rough handling. Response to large local temperature transients, including placing the loadcell on a steel block heated to around 60 C, was small and recovery rapid. This indicated that the "dummy" spring system was doing its job well.

It was decided that Loadcell #9 was sufficiently stable to use on the final towing system. Aluminium mounting studs were made to ensure that no temperature drift would be

introduced by the mounting arrangements. To ensure that knocks would not upset calibration values in service, a small drop of penetrating adhesive was introduced to each can. This had little observed effect on the output.

A new, miniaturised conditioning circuit was built and hosed in a sealed box. The box dimensions are approximately 90x50x25mm. The leads from the loadcell to the circuit are 200mm long to allow the box to be mounted remotely. Power supply and output connections are through a 2 metre shielded cable. This cable could be as long as required by any particular installation.

In Operation

The loadcell was mounted on the towing system and was calibrated in-situ using a range of weights spanning the load-range. Linearity was better than 0.2% FSO and combined hysteresis and creep less than 0.1% FSO after 3 minutes at 50% load. During the 5 week tank testing series the loadcell was recalibrated a total of 27 times using a standard 10N load measured on a precision Mettler balance. The standard deviation of calibrated zero point represented less than 0.4% FSO. The standard deviation of gain calibrations represented less than 0.9% of the mean value. These excellent figures were obtained despite temperature ambient fluctuations estimated at over 10 C, constant use, frequent removal, and several severe shock loads during development of the rig control systems. The high overload capacity of the cell meant that new control methods could be developed without worries about damaging the loadcell, and meant that it survived where a conventional cell would almost certainly have been damaged.

The stiffness of the cell, although well below the original target was sufficient to raise the first resonant mode within the towing system drive train to over 350 Hz. The

limiting factor for the towing configuration implemented turned out to be the natural frequency of the model mass in conjunction with the loadcell. Even with a model mass of 30kg, a natural frequency of over 65Hz was achieved.

In conclusion, the Loadcell #9 proved to be excellent in service, drift was acceptable and the high overload capacity proved to be an very useful feature.

5.8.4 Development Considerations

It must be stated here that Loadcell #9 is still only a development prototype. Much work still remains to be done to improve the performance figures further, increasing the stiffness back towards the original target and to reduce size and machining/assembly time. A number of further developments have been considered. Perhaps the best way to reduce size would be to integrate the receiver grating and photodiodes. Microfabrication techniques could be used to generate a photodiode array in the form of a grating, this would allow dramatic reduction in size of the opto cans and would confer other advantages such as an apparent improvement in collimation from the single emitter and improved current transfer ratio. The photodiode conditioning circuitry would also be on this substrate potentially yielding S/N ration increases. The mechanical layout is open to significant size reduction, although the depth of the spring systems would be maintained to keep the high degree of off axis load isolation. The conditioning circuitry still uses many discrete components, integration here would also yield benefits in terms of drift, S/N ratio and size.

It should be noted that apart from the active emitter drive circuit the temperature stability of the cell is conferred entirely by the mechanical configuration. Some form of active temperature compensation circuitry could yield significant benefits.

In conclusion, there are many possible avenues for continued development. Many of these involve microfabrication techniques and as such could only be carried out if substantial funding was available.

5.9 Discussion of Development Approach/Methodology

During the development programme many corners were cut and stones left unturned. A this stage a critical review of the development approach and methodology used is required.

Loadcell development was originally seen as a peripheral element to the PhD project. Thus there was pressure to produce a working loadcell as rapidly as possible. This rushed approach had a number of advantages and drawbacks.

The over-riding shortfall was the lack of availability of a suitable testing environment. With hindsight it may have been worth the effort involved to set up my own facilities. This could have taken the form of a simple insulated box with crude temperature control and a facility for applying loads to the test cell externally. However, the qualitative methods and intuition- based trouble shooting used gave very rapid appraisal of each new design. The short prototype turn-around times achieved, typically less than 48 hours, kept the ball and ideas rolling. Due to the very small effects that led to the large output drift ranges, the assumption that detailed quantitative testing would have been of use is open to doubt. However, the good thermal performance of Loadcell #9 would mean that further development of these concepts would benefit from, or require, detailed testing to assess the relatively smaller effects of design modifications.

A more serious criticism of the development programme was the reluctance to abandon the stainless-steel/twin diaphragm configuration. A more broad-minded approach should have been taken earlier on, with a range of configurations examined before the design development path was chosen. Loadcell #5 should have been assembled.

Criticism may be levelled at the unbending pursuit of the very ambitious stiffness targets. The problem was eventually solved partially due to the relaxation of this specification. However, it should be noted that none of the early prototypes would have performed satisfactorily at the stiffness specification finally achieved. The limits of any technology are most apparent at extremes of application.

In conclusion, the approach used was somewhat un-rigorous and intuitive. This allowed a very large number of prototypes to be tested in a short time. A more broad-minded approach to the configuration used may have cut the total development time.

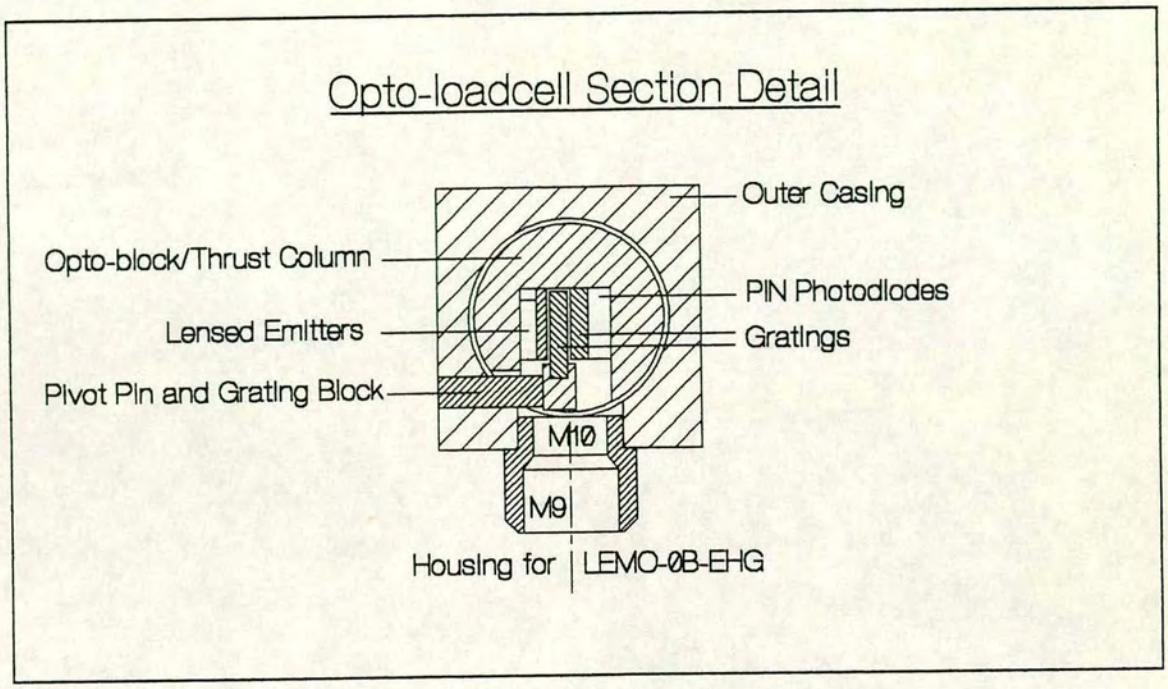

Figure 5.1 Loadcell #1 Cross-section Detail

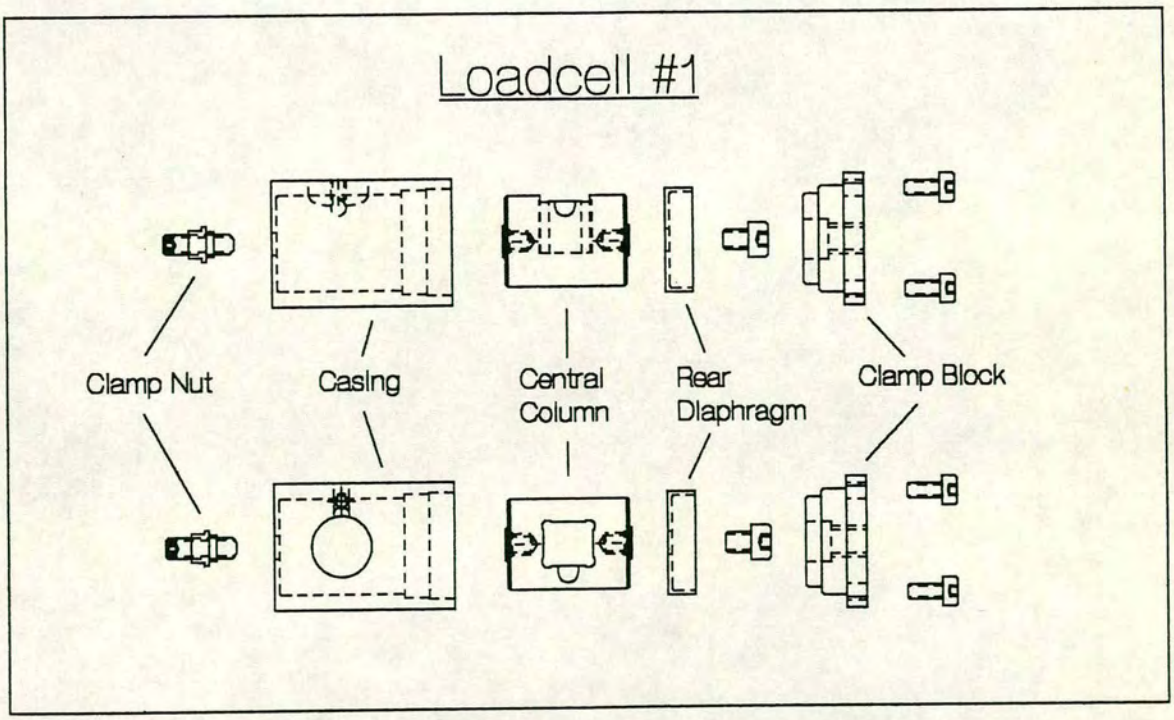

Figure 5.2 Loadcell #1 Component Detail

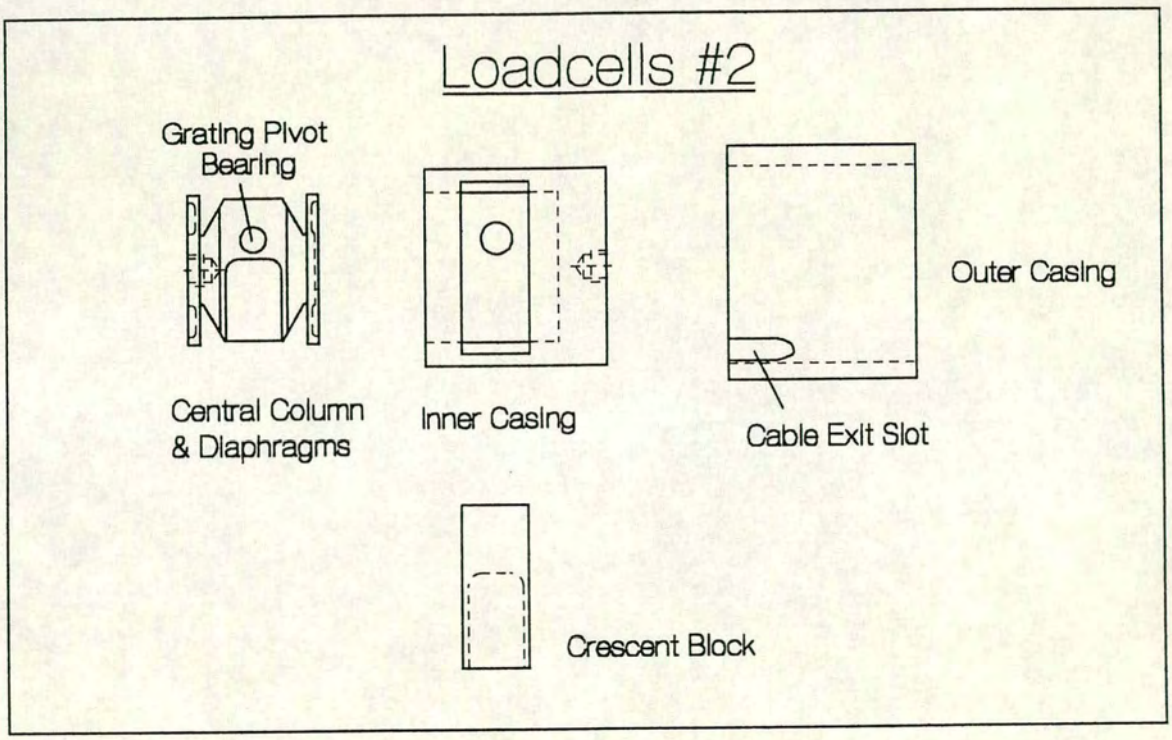

Figure 5.3 Loadcell #2 Component Detail

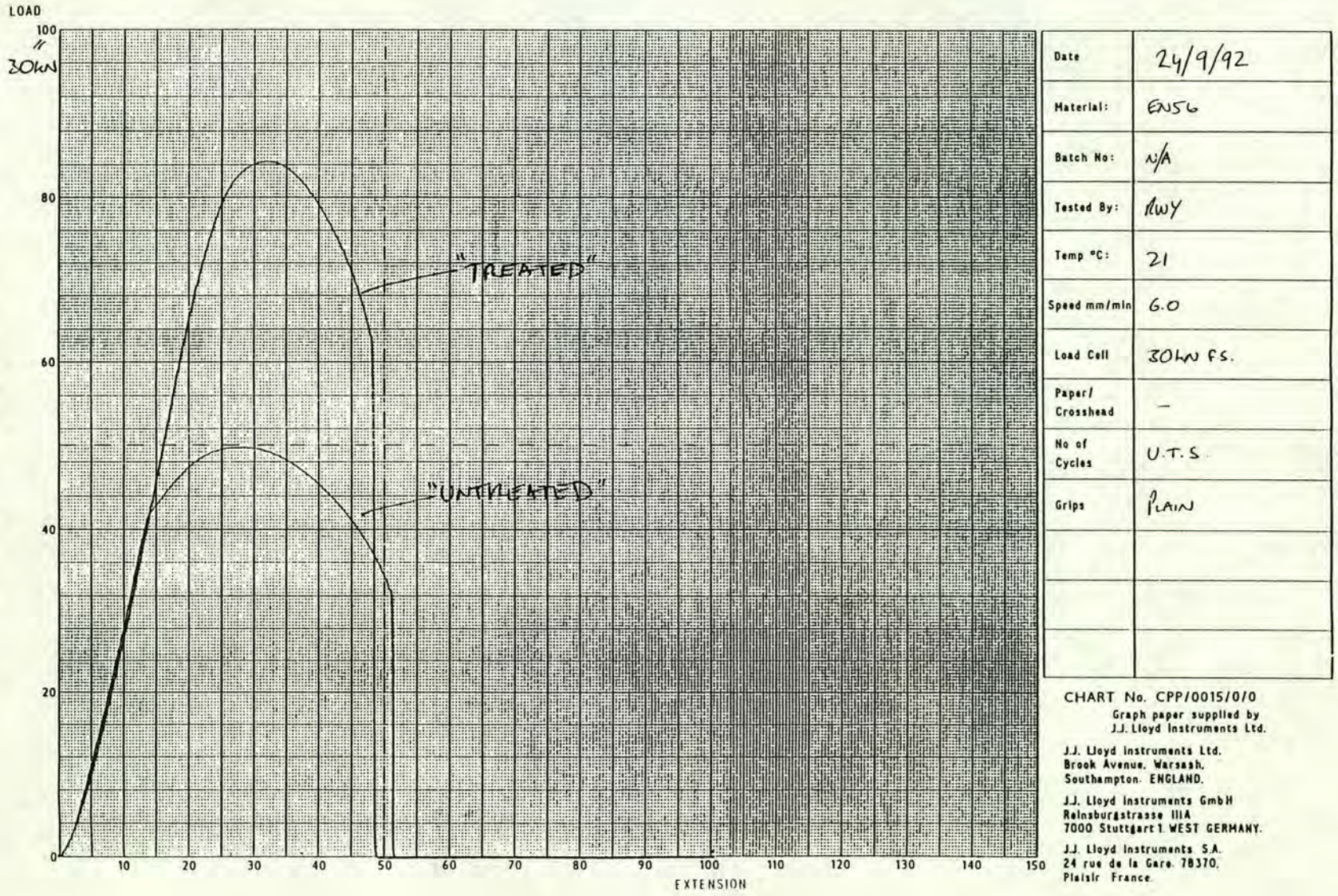

Figure 5.4 Lloyd Tensile Test Results

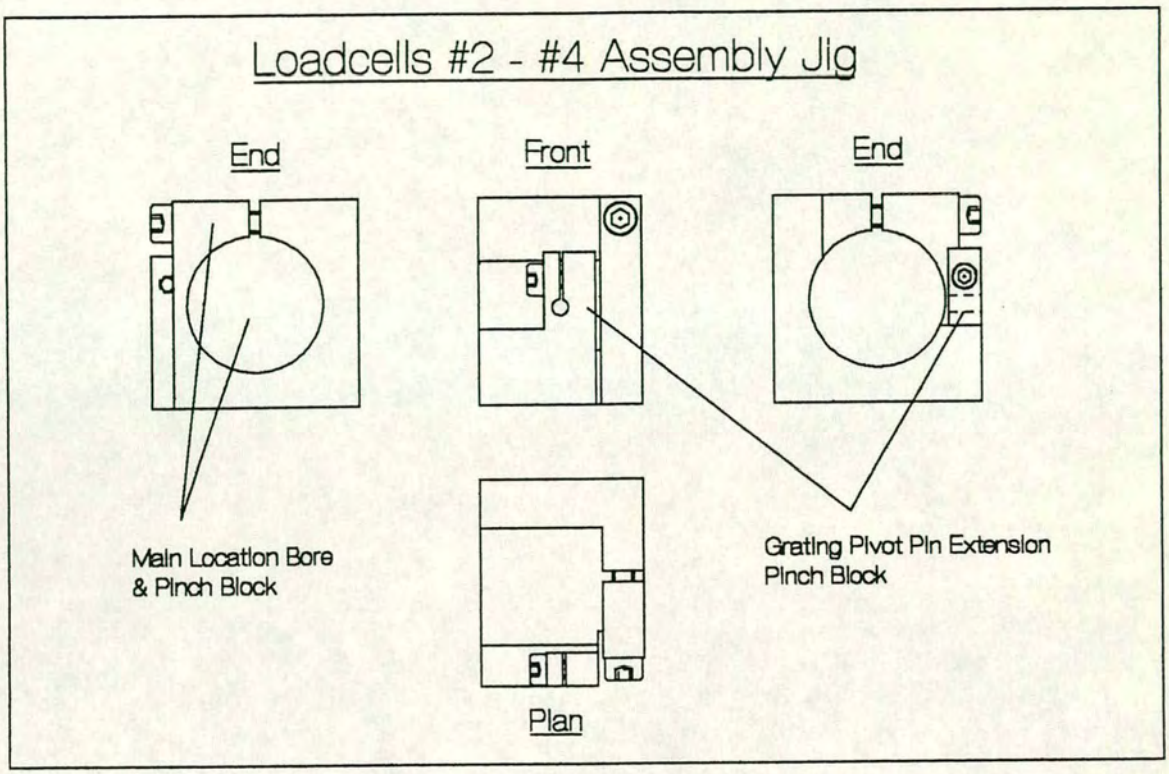

Figure 5.5 Loadcells #2 - #4 Assembly Jig

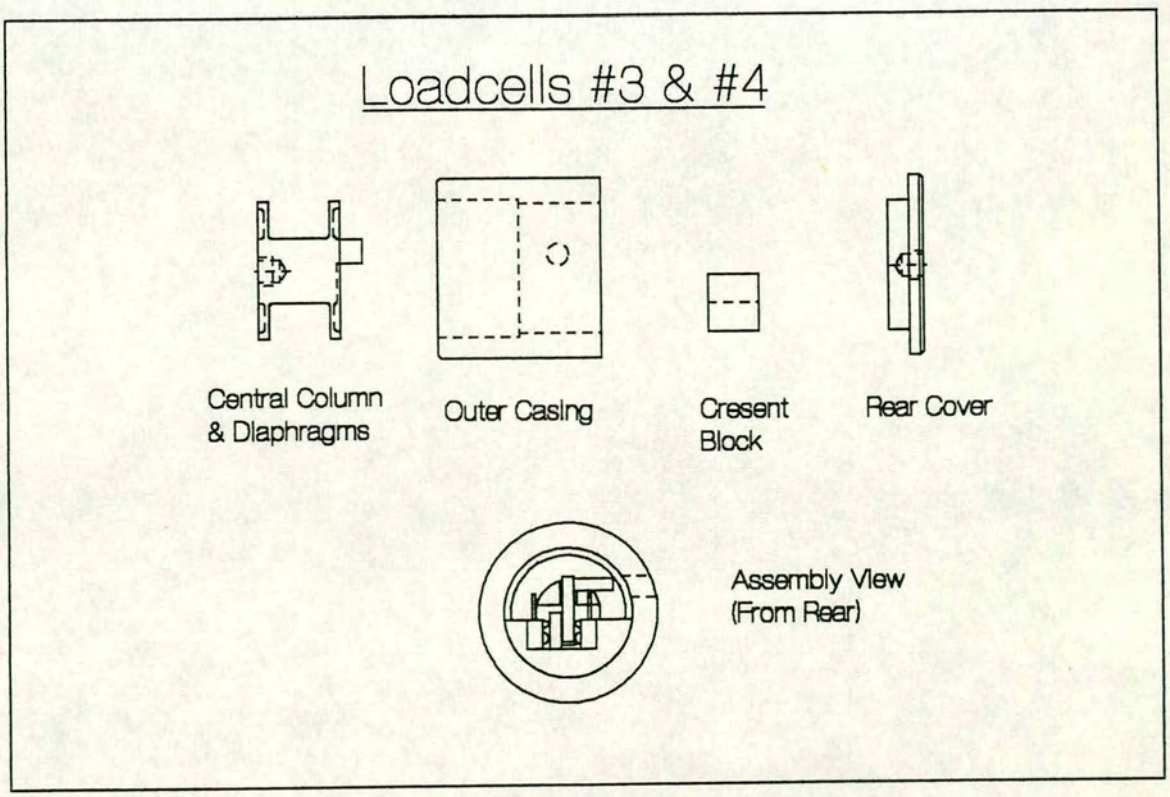

Figure 5.6 Loadcells #3 an #4 Detail

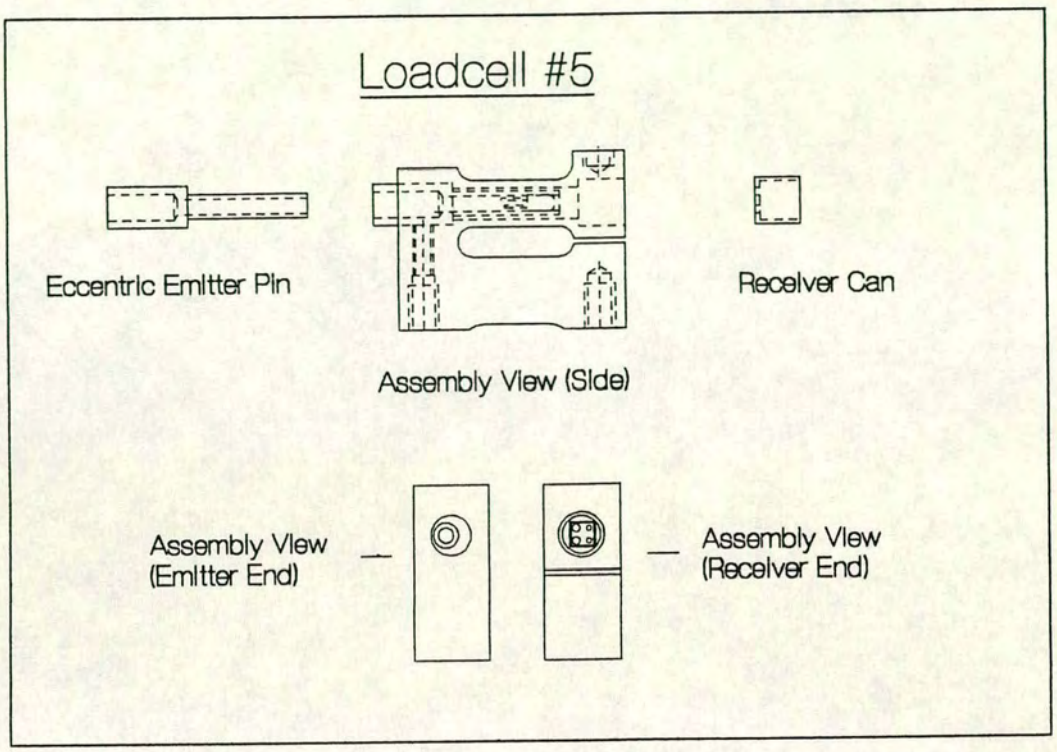

Figure 5.7 Loadcell #5 Detail

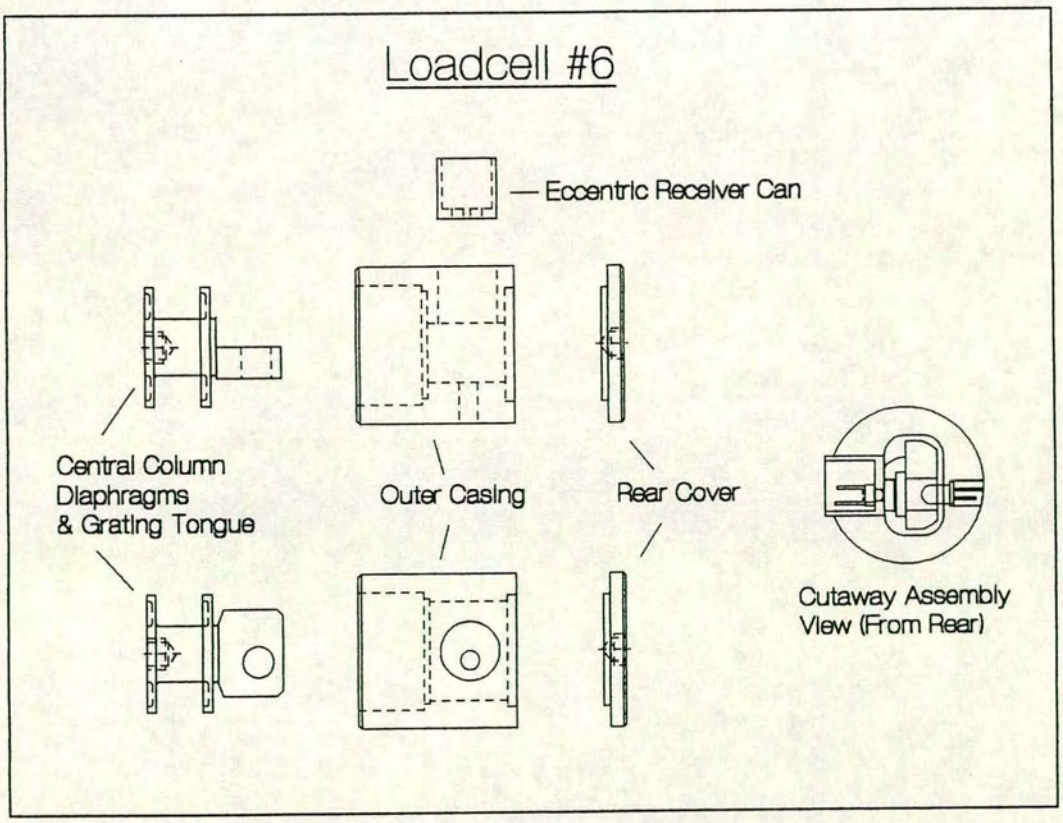

Figure 5.8 Loadcell #6 Detail

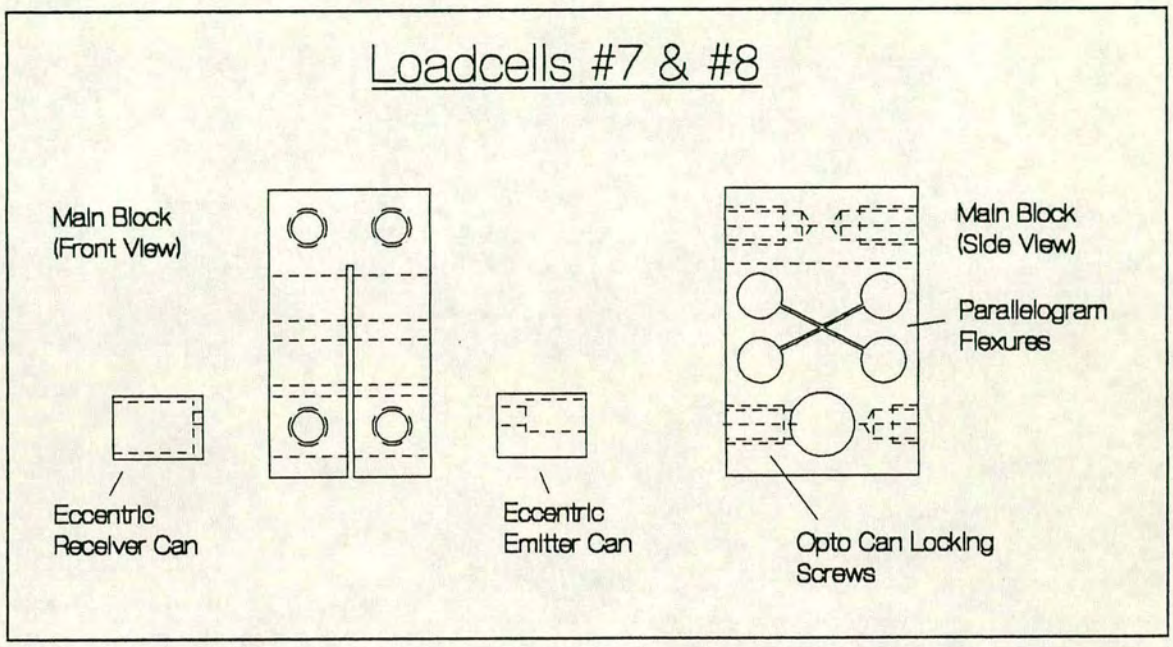

Figure 5.9 Loadcells #7 and #8

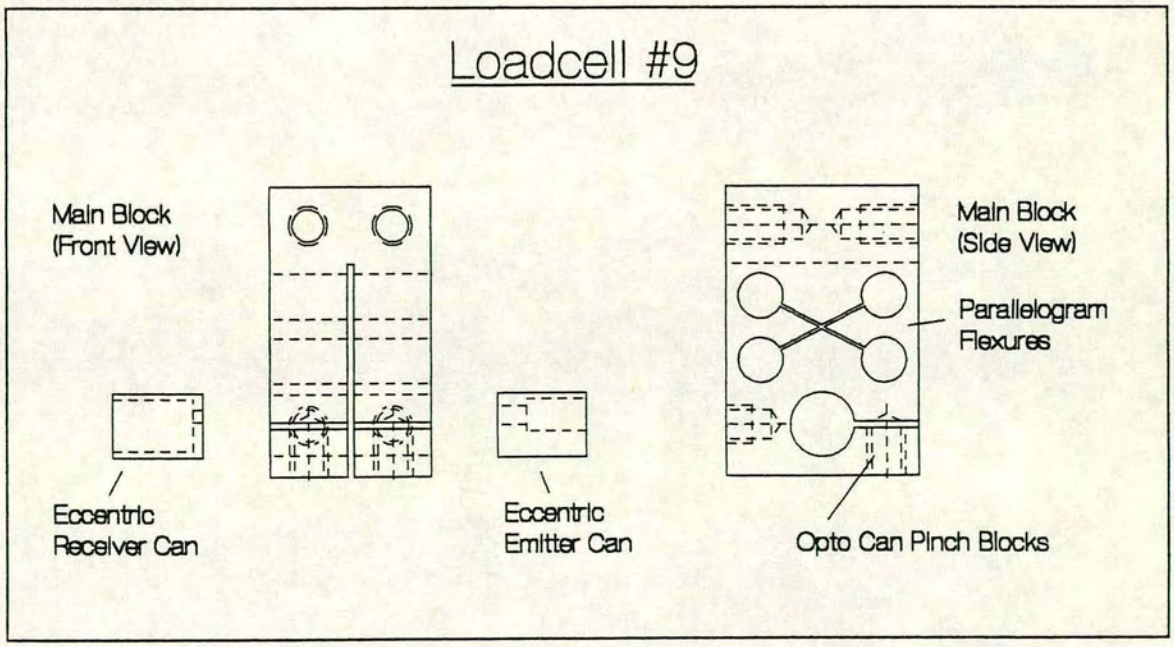

Figure 5.10 Loadcell #9

Chapter 6. Conclusions

6.0 Chapter Summary

This Chapter summarises and concludes Part II of this thesis.

6.1 Project Conclusions

The following conclusions can be drawn from Part II of the thesis:

- Several alternative methods of making a stiff, DC coupled loadcell were evaluated.

- The most promising seemed to be a system based on optical techniques.

- An optical measuring system using the shuttering effect of two parallel gratings was extensively investigated.

- A peak resolution of less than 1 nanometre was achieved.

- Techniques for application of this system to load measurement were devised.

- A series of 9 prototypes were made and evaluated.

- Problems with temperature drift were solved by de-rating stiffness and adopting a mechanical configuration that provides a large degree of automatic temperature compensation.

- All mechanical configurations conferred high overload capacities of between 20 and 80.

- The final loadcell prototype was used extensively in the towing system.

- A large number of calibrations were carried out indicating that the loadcell output was consistent and stable.

- A study of potential future development was carried out.

List of References

[1] Neubert, H.K.P., "Instrument Transducers, Second Edition", Clarendon Press, Oxford 1975.

[2] Dally,J.W.,Riley,W.F.,McConnell, K.G., "Instrumentation for Engineering Measurement, Second Edition", J. Wiley & Sons, New York 1984.

[3] Doebelin, E.O., "Measurement Systems - Application and Design, Third Edition", McGraw-Hill Book Company, New York 1983.

[4] Bolton, W., "Instumentation and Measurement", Newnes, Oxford 1991.

[5] Luxmoore, A.R., "Optical Transducers and Techniques in Engineering Measurement", Applied Science Publishers, London 1983.

[6] Stevenson, J.T.M., Jordan, J.R., "Metrological Gratings and Moire Fringe Detection Methods for Displacement Transducers", IEE Proceedings, Vol.136, Part A, No.5, September 1989.

[7] Timoshenko, S.P., Woinowsky-Krieger, S., "Theory of Plates and Shells, Second Edition", Chapter 3, McGraw-Hill, Tokyo 1959.

[8] Roark, R.J., Young, W.C., "Formulas for Stress and Strain, Fifth Edition", McGraw-Hill Book Company, New York 1982.

[9] Oberg, E., Jones, F.D., Horton, H.L., "Machinery's Handbook, Revised 21st Edition", Industrial Press Inc, New York 1979.

[10] Boyer, H.E., Gall, T.L. (Editors), "Metals Handbook, Desk Edition", American Society for Metals, Ohio 1985.